Oil & Gas Science and Technology – Rev. IFP, Vol. 55 (2000), No. 2, pp. 135-158

Opaque Multiphase Reactors: Experimentation, Modeling and Troubleshooting

M.P. Dudukovic[1]

1 Chemical Reaction Engineering Laboratory (CREL), Department of Chemical Engineering, Washington University, One Brookings Drive, Campus Box 1198, St. Louis, MO 63130-4899 - USA
e-mail: dudu@wuche3.wustl.edu

Résumé — Réacteurs polyphasiques opaques : expérimentation, modélisation et traitement des incidents — Les réacteurs polyphasiques sont largement utilisés dans les industries pétrolière, chimique, pétrochimique, pharmaceutique et métallurgique, aussi bien pour la transformation des matières que pour la réduction de la pollution. La plupart des réacteurs présentant un intérêt industriel (colonnes à bulles avec solides en suspension – à slurry –, lits entraînés – risers – gaz-solide et lits fluidisés, lits bouillonnants et cuves agitées) sont opaques, parce que la phase dispersée occupe une fraction de volume importante. Tous les phénomènes physiques jouant sur la dynamique des fluides de tels systèmes ne sont pas encore entièrement compris. Cela rend extrêmement difficile la prédiction de paramètres importants du procédé, tels que la perte de charge, les profils de vitesse et de rétention, le taux de rétromélange, etc.

Les concepts industriels reposent sur des corrélations, et celles-ci sont sujettes à une grande incertitude dès que l'on s'écarte des conditions d'exploitation des bases de données. Dans la plupart des cas, il serait bienvenu de prévoir les paramètres du procédé en se basant sur des modèles de dynamique des fluides. Cependant, même les meilleurs modèles (ceux qui sont aptes à traiter des récipients et des conduites de grand volume) nécessitent des lois de fermeture pour les termes d'interaction des phases, qui sont encore actuellement incertains et sujets à discussion. Il est donc nécessaire de vérifier ces modèles en mesurant avec précision les grandeurs que l'on souhaite prédire à l'aide de ces modèles, c'est-à-dire les taux et les profils de rétention des différentes phases, les profils de vitesse, le rétromélange, etc. Mais ces systèmes sont opaques, et il est donc impossible de « voir » à l'intérieur, ce qui apparaît comme un cercle vicieux et laisse présager que les prédictions des modèles sont destinées à rester invérifiées.

Heureusement, comme deux importantes et récentes études l'ont montré (Chaouki *et al.*, 1997a, 1997b), des techniques peuvent nous offrir les informations souhaitées. Nous examinons ici deux d'entre elles : la tomographie assistée par rayon gamma (CT) pour la mesure des profils de rétention, et le traçage des particules radioactives assisté par ordinateur (CARPT) pour la mesure des profils de vitesse et des paramètres de rétromélange. Nous montrons comment utiliser ces techniques pour obtenir une information sur les systèmes industriellement intéressants et comportant des catalyseurs en mouvement comme les réacteurs élévateurs (risers) gaz-solide ou gaz-liquide, et les colonnes à bulles gaz-liquide.

L'aptitude des codes CFD *(Computational Fluid Dynamics)* existants à prédire correctement les grandeurs hydrodynamiques observées est également brièvement discutée. Nous abordons ensuite les problèmes de l'écoulement disphasique dans les lits garnis, de l'évolution des techniques expérimentales et des modèles utilisés pour mieux quantifier les paramètres de ces réacteurs. Enfin, l'on évoque les applications des méthodes de traçage pour l'analyse et le traitement des incidents dans les réacteurs industriels.

Mots-clés : colonne à bulles, élévateur, réacteurs agités, réacteur à lit fixe ruisselant, suivi de particules.

Abstract — Opaque Multiphase Reactors: Experimentation, Modeling and Troubleshooting — *Multiphase reactors are widely used in petroleum, chemical, petrochemical, pharmaceutical and metallurgical industries as well as in materials processing and pollution abatement. Most reactors of interest in industrial practice (slurry bubble columns, gas-solid risers and fluidized beds, ebullated beds and stirred tanks) are opaque as they contain a large volume fraction of the dispersed phase. All the physical phenomena that affect the fluid dynamics of such systems are not yet entirely understood. This makes a priori predictions of important process parameters (pressure drop, velocity and holdup profiles, degree of backmixing, etc.) very difficult.*

Industry relies on correlations, and these are prone to great uncertainty as one departs from the operating conditions contained in the available limited data base. Prediction of the needed process parameters based on fundamental fluid dynamic models would be most welcome, yet even the best models (that can treat large vessels or conduits that are of interest) require closure forms for phase interaction terms which are still subject to uncertainty and debate. Hence, there is a need to verify such models; verification can only be accomplished if we measure precisely those quantities that we would like the model to ultimately predict, i.e. *phase holdup and holdup profiles, velocity profiles, backmixing, etc. However, the systems are opaque and we cannot "see" into them, and so it seems that a vicious circle has been closed and that model predictions are destined to remain unchecked.*

Fortunately, as two extensive recent reviews point out (Chaouki et al., *1997a, 1997b) there are techniques which can provide us with the desired information. In this paper, we review two of them: gamma ray assisted tomography (CT) for measurement of holdup profiles and computer aided radioactive particle tracking (CARPT) for measurement of velocity profiles and backmixing parameters. We then show how these techniques can be used to obtain information in systems with moving catalysts of industrial interest such as gas-solid riser, liquid-solid riser and gas-liquid bubble column.*

The ability of the available CFD (Computational Fluid Dynamics) codes to correctly predict the observed hydrodynamic quantities is also briefly discussed. We then address the issue of two-phase flow in packed beds and the evolution of the experimental techniques and models used to quantify these reactors better. Finally, troubleshooting on industrial scale reactors and use of tracer methods to accomplish this are briefly mentioned.

Keywords: bubble columns, risers, stirred tanks, trickle beds, particle tracking.

INTRODUCTION

In diverse industries such as chemical processing, petroleum refining, food production, pharmaceuticals and specialty materials processing, etc., multiphase opaque systems play a dominant role. The systems encountered vary from gas-solid flows (bubbling and churn-turbulent fluidized beds, dense risers, pneumatic conveying, etc.), liquid-solid flows (fluidized beds, risers, etc.), gas-liquid flows (bubble columns, gas-lift reactors, evaporators, etc.), gas-liquid-solid flows (slurries in agitated vessels, bubble columns, ebullated beds). When such multiphase systems are used as reactors it is increasingly necessary to determine the phase holdup profile in such reactors and describe the flow pattern and its deviation from the usually assumed ideal flow patterns, *e.g.* plug flow or perfect mixing. The large volume fraction of the dispersed phase, and/or churn-turbulent flow conditions, make the above described multiphase flows opaque and inaccessible to probing with instrumentation that is customarily employed in single-phase fluid mechanics (*e.g.* particle image velocimetry (PIV), laser doppler velocimetry (LDV), hot wire anemometry (HWA), etc.). Since the theory of such flows with highly concentrated dispersed phase in churn-turbulent conditions is not fully developed, it is both prudent and necessary to learn more about them *via* experimentation.

An ideal experimental system should have the following features:

– high spatial and temporal resolution for noninvasive measurement of holdup (volume fraction) distribution across the desired planes in the flow field;
– high temporal and spatial resolution for the velocity vector field of all phases;
– be capable of providing snapshots of the flow, as well as the time history of it, over the whole process unit in equipment of different scales with and without internals.

A selection of papers contributed by experts on noninvasive monitoring of multiphase flows (Chaouki *et al.*, 1997a) reveals that such an ideal all encompassing experimental system has not yet been invented. Regarding density profile measurements, one often sacrifices spatial for temporal resolution and *vice versa*: identifying the volume

fraction profile of more than two phases remains difficult, getting accurate measurement of instantaneous phase velocities and slip velocities in opaque flows seems still out of reach. Mapping the flow field over the whole vessel is also quite difficult. While many new techniques that are being explored (*e.g.* NMR—nuclear magnetic resonance—ultrasonics, electric impedance tomography, etc.) show promise, they cannot as yet provide the needed information in large vessels with opaque flows. The best and most robust techniques available still rely on attenuation of signals emitted from a radioactive source (Chaouki et *al*., 1997a, 1997b). A rather detailed review of the principles, advantages and disadvantages of various tomographic and velocimetry techniques for multiphase flows was recently provided by Chaouki *et al.* (1997b).

The state of modeling of multiphase flows with concentrated dispersed phase (which are opaque), is not any more advanced than the instrumentation available for measurement of fluid dynamic quantities of such flows. However, availability of robust algorithms and of the flexible multifluid model (*e.g*. CFDLIB of Los Alamos, FLUENT, CF, etc.) makes the use of these codes attractive. Today they are at the state that velocity and holdup profiles can be computed in both two-dimensional (2D) and three-dimensional (3D) enclosures but the accuracy of such computations in multiphase flows remains to be determined due to the uncertainty involved in the description of physics of phase interactions.

Advanced modeling of multiphase reactors for design, scale-up and performance enhancement purposes requires a more detailed description of the flow pattern than the currently used ideal flow assumptions (*e.g.* plug flow or perfect mixing). Since CFD at present cannot provide the holdup and velocity fields with certainty, it is necessary to develop improved reactor models based on experimental evidence and enhanced understanding of the physical phenomena occurring in these systems. In our Chemical Reaction Engineering Laboratory (CREL) we have undertaken the task of developing the experimental techniques needed for evaluation of holdup and velocity in multiphase reactors of interest to industry. The generated data base serves two main purposes: it provides the physical basis for development of improved models for multiphase reactor flow patterns and evaluation of their parameters, and it yields the information needed for verification of CFD multiphase codes. Such flow visualization techniques are also very convenient for assessing the role of internals and novel design configurations on the flow structure. Discussion of the means by which needed experimental data can be collected, and a review of the type of data that is obtainable and its utility, are the primary topics of this brief outline of the work performed in CREL. Due to space limitations no attempt is made to provide a comprehensible review of the activities of many other distinguished laboratories.

1 EXPERIMENTAL TECHNIQUES FOR FLOW VISUALIZATION IN OPAQUE SYSTEMS

1.1 Gamma Ray Computed Tomography

To measure the phase holdup distribution at any desired cross-section of the column we have implemented a gamma source based fan beam type CT unit *(Fig. 1)*. A collimated encapsulated hard source (100 mCi of Cs-137) is positioned opposite eleven 2" (0.05 m) sodium iodide detectors in a fan beam arrangement. The lead collimators in front of the detectors have manufactured slits and the lead assembly can move so as to allow repeated use of the same detectors for additional projections. A 360˚ scan can be executed at any desired axial location and columns from 1 to 18" in (0.02-0.45 m) diameter can be scanned in the current configuration. The principle of computed tomography is simple. From the measured attenuation of the beams of radiation through the two-phase mixture (projections) we calculate, due to the different attenuations by each phase, the distribution of phases in the cross-section that was scanned. In our CREL CT unit we achieve 3465 to 4000 projections and have a spatial resolution of 5 mm and density resolution of 0.04 g/cm^3. We need a long time to scan the cross-section (about 45 min) and, hence, can only achieve the time-averaged density distribution. Details of the CT unit are available elsewhere (Kumar *et al*., 1995; Kumar and Dudukovic, 1997; Kumar, Moslemian and Dudukovic, 1997). Among the suggested techniques for reconstruction, *e.g.* convolution or filtered back projection, algebraic reconstruction and estimation-maximization algorithms (E-M), we have found the E-M algorithm to be the best (Kumar and Dudukovic, 1997). All CT hardware and software was developed in house.

When nearly symmetrical density profiles are encountered, the radial density profiles are calculated and displayed. The spatial resolution of this type of scanner can be improved further with smaller scintillation detectors and a stronger source. Moreover, reasonable temporal resolution could be obtained by going to a 4-th generation scanner (with only the source rotating and detectors being stagnant). All these improvements would require considerable investment. The present scanner is quite adequate for obtaining two-dimensional density profiles in columns from 1 to 18 in (0.02-0.45 m) in diameter operated with gas-liquid or liquid-solid flows. Additional experimental tomographic techniques with potentially better temporal resolution based on X-ray or positron emission tomography, nuclear magnetic resonance, electrical impedance tomography, and optical, microwave and ultrasonic tomography are being explored and their limitations have been carefully reviewed (Chaouki *et al*., 1997).

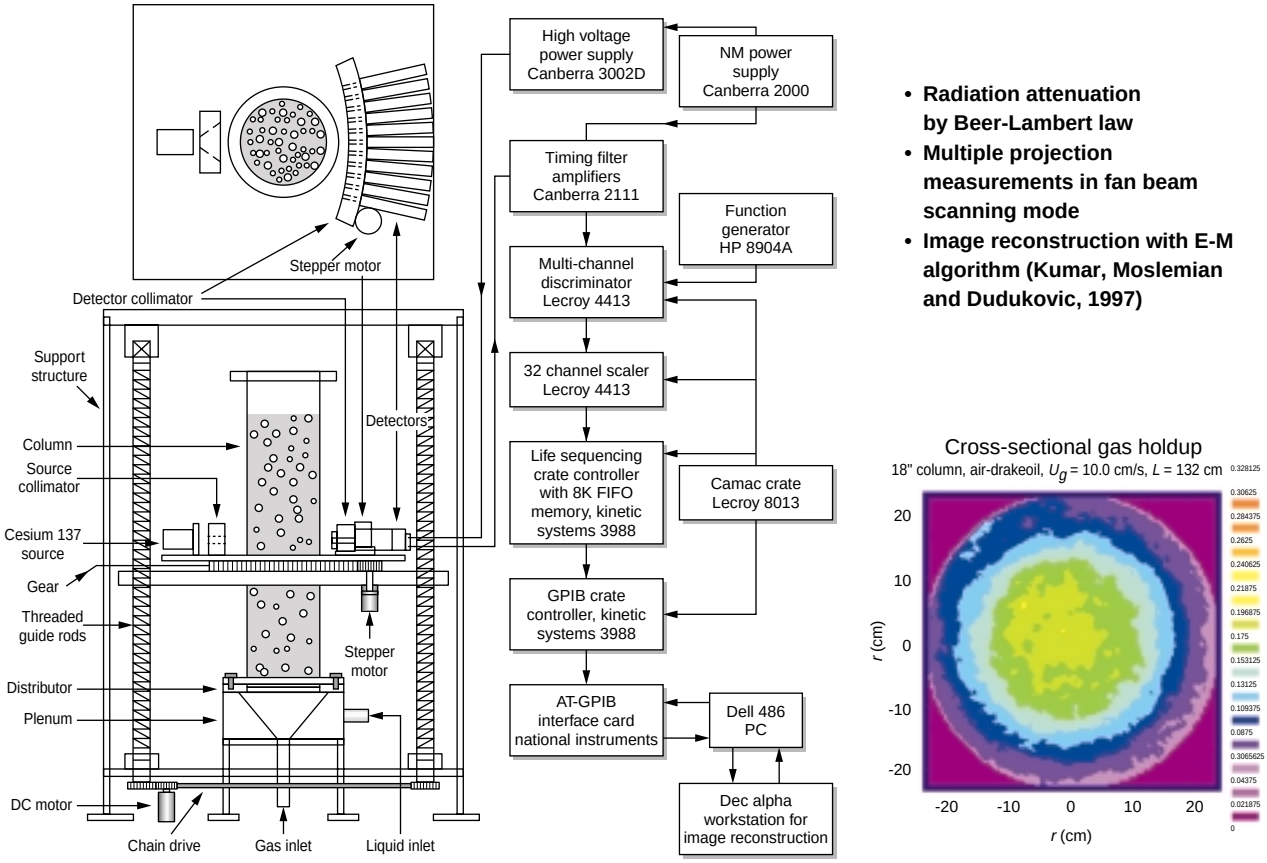

Figure 1

Gamma ray computer tomography setup at CREL (inset shows gas holdup distribution in 14 cm diameter bubble column).

1.2 Computer Aided Radioactive Particle Tracking (CARPT)

The computer aided radioactive particle tracking, or simply radioactive particle tracking (RPT), consists of introducing into the flow field a single radioactive particle (gamma ray emitter) of the same size and density as the solid particles to be traced, or a neutrally buoyant particle if liquid is traced (Devanathan, Moslemian and Dudukovic, 1990). The column (bubble column, slurry bubble column, fluidized bed, ebullated bed, etc.) is then operated at steady superficial velocities, while the position of this single radioactive particle is detected and monitored in time by an array of 2×2" sodium iodide scintillation detectors strategically located all around the column. Precalibration at operating conditions of interest establishes the relationship between radiation intensity detected at each detector and particle position. The first modern version of CARPT was introduced by Lin, Chen and Chao (1985) in studies of solids motion in gas fluidized beds and was further perfected by Devanathan, Moslemian and Dudukovic (1990), Larachi, Kennedy and Chaouki (1995), Yang, Devanathan and Dudukovic (1993) and Degaleesan (1997) who also adopted it for use in bubble columns and ebullated beds.

When solids motion is monitored in ebullated beds, fluidized beds or slurries, a particle of the same size and density as the solids in the system is prepared. For monitoring of liquid motion a neutrally buoyant particle is made (Devanathan, Moslemian and Dudukovic, 1990). For example, a polypropylene bead of about 2 mm in diameter is hollowed out, a small amount of scandium 46 is inserted, and a polypropylene plug is put in place, so that the density of the composite particle consisting of polypropylene, scandium and air gap equals that of the liquid. Thin film metallic coating assures that bubbles do not preferentially adhere to the particle. An array of scintillation detectors is located around the column *(Fig. 2)*. In our case up to 32 NaI 2" detectors are used. The detectors are calibrated *in situ* with the tracer particle to be used to get the counts-positions maps. Conventionally, CARPT calibration was done by positioning

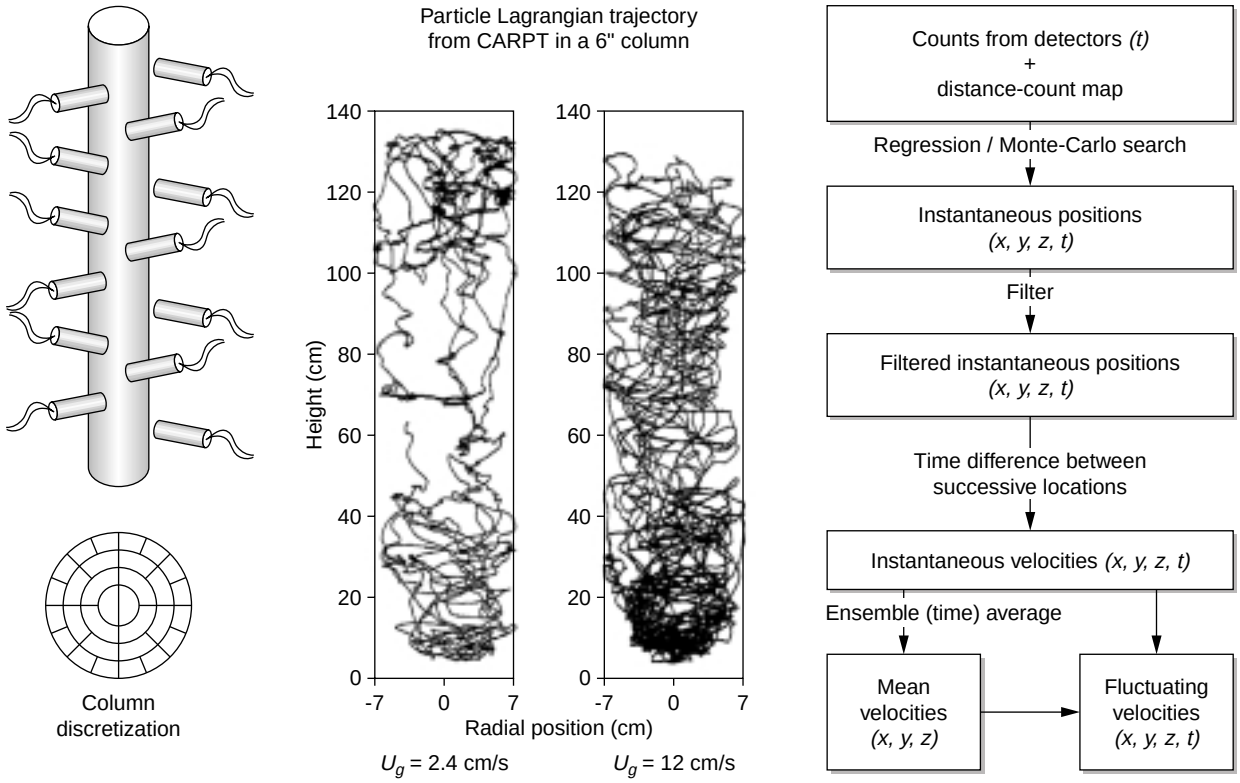

Figure 2

CARPT schematic, position reconstruction and post-processing (inset shows particle trajectory during 100 s in bubbly and churn-turbulent flow).

the tracer particle (usually Sc-46 of 250 μCi strength was used) at about 1000 known locations and recording the counts obtained at each detector. Various ways of doing this have been described (Devanathan, 1991; Degaleesan, 1997). An alternative way of constructing distance-count maps is *via* modeling of particle emission of photons and transmission and subsequent detection at the detectors. The Monte-Carlo method (Larachi *et al*., 1994; Gupta, 1998) in which the photon histories are tracked in their flight from the source, through the attenuating medium and their final detection (or lack of it) at the detector can be used for this purpose. Thus, both the geometry and radiation effects are accounted for in estimation of the detector efficiencies in capturing and recording the photons. This involves evaluation of the complex three-dimensional integrals which are evaluated using the Monte-Carlo approach by sampling modeled photon histories over many directions of their flight from the source. Once calibration is complete, the tracer particle is let loose in the system and the operating conditions are controlled and kept constant for many hours while the particle is tracked. A regression, least squares method is used to evaluate the position of the particle. Sampling frequency is adjusted to assure good accuracy. Typically, it is selected at 50 Hz for bubble columns since the finite size particle used as tracer cannot capture motion of frequencies above 25 Hz (Degaleesan, 1997). With the introduction of wavelet-based filtering to eliminate some of the noise introduced by the statistical nature of the gamma source (Degaleesan, 1997) particle position can be located within a sphere of uncertainty of less than 5 mm in columns as large as 18" in (0.45 m) diameter and 8 ft (2.43 m) tall. Most importantly, the spurious velocity of a stagnant particle can be reduced to less than a percent of the typical velocity encountered in the system (Larachi *et al*., 1997).

The principle of CARPT and processing of the information generated is described in Figure 2. It is important to note that CARPT noninvasively provides the three-dimensional velocity field in the whole column. The whole column is divided into cells and particle position at each sampling time is identified and assigned to a cell. From filtered particle positions at subsequent sampling times instantaneous velocity is calculated and assigned to a cell that

contains the mean particle position between two successive locations. The ensemble average velocities for each cell in the column are directly comparable to ensemble average velocities of the fluid dynamic codes. Moreover, *via* the ergodic hypothesis, these ensemble averages represent time-averaged velocities. The difference between instantaneous and average velocity for each cell allows calculation of RMS velocities and other flow characterization and turbulence parameters such as normal and shear Reynolds stresses, kinetic energy of the flow due to fluctuating velocity, etc.

Clearly, CARPT has both spatial and temporal limitations. The error resulting from the statistical nature of gamma radiation and fluctuating volume fraction in the field of view between the detectors and the tracer particle emitting gamma radiation is taken care of by calibration at *in situ* conditions and by subsequent filtering. Upon such a procedure the radioactive particle kept at a fixed position has negligible RMS velocities and the sphere of uncertainty in identifying the position of the particle is smaller than 4 mm at sampling frequencies of 50 Hz. Particle trajectories can be followed in principle with sampling frequencies up to 500 Hz. The detailed discussion of the error is presented by Larachi *et al.* (1997) and Degaleesan (1997). An error is also caused by discretization of the space occupied by the column into cells of finite size for the purposes of assigning particle positions. Improved statistics are obtained by having frequent particle visits to each cell, improved spatial resolution requires small cells, which in turn leads to excessive running times. Hence, a compromise is reached.

Since the radioactive particle is of the same size and density as the solids to be traced no additional errors are introduced in tracing solids flow. However, for tracing the liquid in gas-liquid flows a neutrally buoyant particle (often 2 mm in size) is used. Evaluation of its motion in a turbulent field, using Meek's equation (1972), shows that the particle follows liquid eddies up to frequencies of 25 Hz. Smaller eddies do not have the size or energy to impact the particle trajectory. Therefore, sampling frequencies of 50 Hz were considered adequate for most multiphase flows studied by CARPT.

The quantities computed from CARPT experiments are shown in Table 1. Lagrangian particle trajectories and velocities are subject to the previously discussed uncertainties due to the statistical nature of multiphase flow and gamma radiation. However, Lagrangian statistics are very reproducible. Ensemble average velocities are readily obtained and taken to represent the velocities at the center of each "cell". Fluctuating velocity components, in the Eulerian sense, can now be derived as well as all the components of the normal and shear stresses and the kinetic energy of the flow due to velocity fluctuations. Most importantly, CARPT allows us to evaluate the components of the diffusivity tensor *via* first principles since the collected data is Lagrangian in nature.

TABLE 1

Quantities calculated from CARPT data

For the entire three-dimensional flow field:

- Lagrangian velocities
- Ensemble/time-averaged velocities
- Turbulent Reynols stresses:

Normal: $\overline{u_r'u_r'}$, $\overline{u_\theta'u_\theta'}$, $\overline{u_z'u_z'}$

Shear: $\overline{u_r'u_\theta'}$, $\overline{u_r'u_z'}$, $\overline{u_z'u_\theta'}$

- Turbulent kinetic energy: $k = \frac{1}{2}\left(\overline{u_r'^2} + \overline{u_\theta'^2} + \overline{u_z'^2}\right)$

- Turbulent eddy diffusivities:

Radial: $D_{rr}(t) = \frac{1}{2}\frac{d}{dt}\overline{y_r^2(t)} = \int_o^t \overline{v_r'(t)v_r'(\tau)}\,d\tau = \int_o^t R_{rr}(\tau)\,d\tau$

Axial: $D_{zz}(t) = \frac{1}{2}\frac{d}{dt}\overline{y_z^2(t)}$

$$= \int_o^t \left\{ \overline{\frac{\partial u_z}{\partial r}\,\middle|\, y_r(t')\left(\int_o^{t'} v_z'(t)\,v_z'(\tau)\,d\tau\right)} + \overline{v_z'(t)v'} \right.$$

$$= \int_o^t \overline{\frac{\partial u_z}{\partial r}\,\middle|\, y_r(t')\left(\int_o^{t'} R_{rz}(\tau)\,d\tau\right)}\,dt' + \int_o^t R_{zz}(t')\,dt'$$

1.3 Use of CARPT-CT Results in Reactor Modeling

In order to improve our understanding of the flow pattern and backmixing, CARPT data has been acquired by various research groups in fluidized beds (Moslemian, Chen and Chao, 1989), in bubble columns (Devanathan, Moslemian and Dudukovic, 1990; Degaleesan, 1997), slurries (Grevskott *et al*., 1996), spouted beds (Roy *et al*., 1999) and ebullated beds (Limtrakul, 1996). Here we briefly review how CARPT-CT results contribute to establishing more accurate flow pattern models for several multiphase reactors such as bubble columns, risers, etc. Then, we address the ability of CFD codes to predict the observed flow patterns.

2 BUBBLE COLUMNS

Bubble columns, due to their good heat transfer properties and relative ease of construction and operation, are reactors of choice for a number of industries and are expected to become especially important in the future in large scale conversion of natural gas and syngas to fuels and chemicals. It is this future use of bubble columns that will severely test the current know-how applied to their design and operation. Hence, a more fundamental understanding of the fluid

dynamics and transport processes in bubble columns is highly desirable in order to reduce the uncertainties in scale-up and optimize the design and performance of these reactors. Molecular scale investigations are needed to properly understand the catalysts and the chemistry of the gas conversion processes. Bubble scale phenomena are essential to understand the transport of gaseous reactant to the catalyst particle where reaction with the liquid reactant takes place. Moreover, bubble scale phenomena affect the global phase holdup and velocity distribution.

Reactor scale phenomena of gas holdup distribution, liquid recirculation, liquid and gas backmixing are critical in sizing the reactor properly for the desired performance and in achieving optimal performance. These have been the focus of our studies.

The state of the art in design and modeling of bubble columns until a few years ago relied solely on the use of ideal flow patterns (*e.g.* perfectly mixed liquid and plug flow of gas) or on the use of the axial dispersion model (ADM). The use of ideal flow patterns can lead to serious overdesign, and the uncertainty of the axial dispersion coefficients precludes a more accurate design based on ADM. All these models represent the crudest description of the flow pattern in bubble columns and do not account for actual fluid dynamics of the system. The need for rapid scale-up and optimal commercialization of bubble columns for gas conversion processes, and the need to operate in the churn-turbulent regime, which was largely unknown, necessitated an improved understanding and quantification of fluid dynamics and transport in bubble columns. In response to this need the slurry bubble column reactor (SBCR) hydrodynamics initiative has been undertaken in the US as well as in the European community. As part of this program we at CREL undertook the following tasks:

- development of instrumentation for measurement of velocities and holdups throughout the column;
- development of data base for evaluation of parameters in physically based engineering models and for CFD testing;
- development of such improved engineering models;
- testing of old and new models with tracer data taken at the Advanced Fuels Development Unit (AFDU) in LaPorte, Texas;
- testing and identification of suitable CFD models for bubble columns.

A standard bubble column is typically a cylindrical vessel operated at superficial gas velocities that exceed those of the liquid by at least an order of magnitude. For very small catalyst particles the slurry (*e.g.* solids suspension in liquid) can be treated as pseudo-homogeneous. The gas dynamics dictates the fluid motion and mixing in the column. The current representation of this complex flow pattern by the axial dispersion model attempts to lump the description of too many physical phenomena into a single dispersion coefficient which cannot be done in a precise manner. Hence, we needed to understand and quantify the physical phenomena occurring on the column scale, and this necessitated experimental observations of holdup and velocity distributions throughout the column. Since bubble column flows are buoyancy driven flows, the quantification of the gas holdup cross-sectional profiles as a function of operating conditions is important. To accomplish this we have used our gamma ray computer tomography system. It enables us to monitor the averaged gas holdup profiles in various cross-sections of the column at different superficial gas velocities and in different diameter columns. Due to almost axisymmetric distribution of the gas, azimuthal averaging yields radial gas holdup profiles which are frequently pretty much height invariant after a distance of 1 to 1.5 diameters from the distributor. The radial gas holdup distribution drives the liquid recirculation by buoyancy forces. When the gas superficial velocity is low, the gas holdup profile is relatively flat in bubbly flows, while in churn-turbulent flow, at high gas superficial velocity, the gas holdup profile becomes almost parabolic. In any event, the gas holdup profile can be represented by a power law form in terms of dimensionless radius.

To measure the liquid velocities throughout the bubble columns of different diameters operated at various superficial velocities we used our CARPT facility with a neutrally buoyant single tracer particle containing Sc-46 of activity ranging from 200 to 500 μCi depending on the diameter of the column. Column diameters from 14 to 44 cm were studied. After filtering the position data to remove the fluctuations of the gamma source, instantaneous velocities, ensemble average velocities and cross-correlations of various fluctuations are calculated for all the column components. For example, the inspection of the tracer particle trajectory in bubbly flow during 100 s establishes that it is much shorter than in churn-turbulent flow during the same time interval *(Fig. 2)*. Runs of up to 36 h in duration were implemented to assure good statistics.

The projection of the ensemble average liquid velocity vector field, as evaluated by CARPT, on four vertical planes at different angles θ is shown in Figure 3 for a 14 cm diameter bubble column. The column is operated in churn-turbulent flow at superficial gas velocity of 12 cm/s with a perforated plate distributor with 61 holes 0,04 cm in diameter. It is evident that, in a vertically aligned column with a symmetric distributor, the time-average flow pattern is highly symmetric and consists of a single recirculating cell with liquid rising in the middle of the column and flowing down by the walls. Except for the distributor region and the top disengagement zone (each approximately one column diameter high), the liquid ensemble average flow seems fully developed in the sense that time-averaged azimuthal and radial velocities are negligibly small compared to the axial ones throughout most of the column. Only in the distributor region, where roll cells feeding the liquid towards

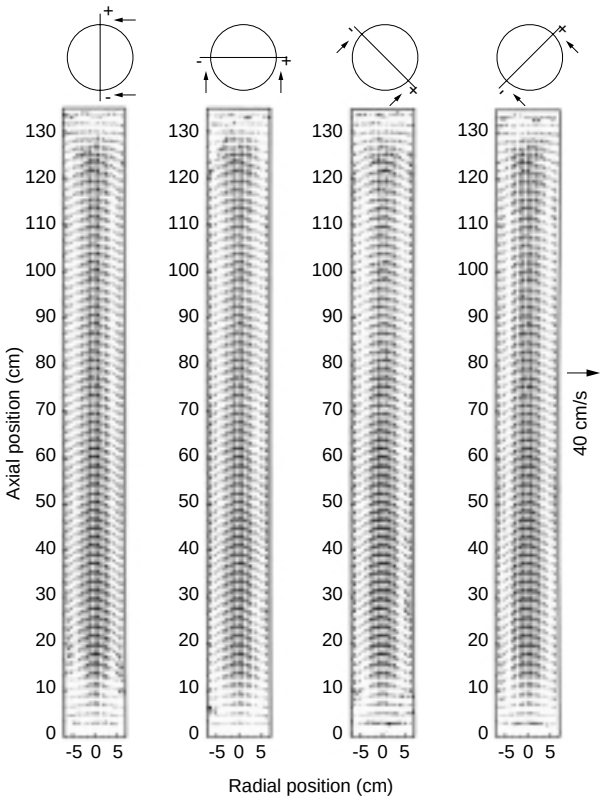

Figure 3

Velocity vector plots for column diameter of 14 cm. Distributor: perforated plate (6A), U_G = 12 cm/s (longitudinal view). (From Degaleesan, 1997.)

the center are observed, and in the gas disengagement zone,where a radially outward fountain type flow is observed, does one encounter significant non-zero azimuthal and radial ensemble average velocities. Degaleesan (1997) has recently demonstrated that this flow pattern prevails in all column diameters studied, up to 44 cm, and she discussed in detail the effects of the distributor. The axial ensemble average liquid velocity profiles can be averaged along that portion of the column height where radial velocities are negligible and are presented in Figure 4 as a function of column diameter and gas superficial velocity together with azimuthally averaged gas holdup profiles. Increased liquid recirculation at higher superficial gas velocities is driven by increasingly steep gas holdup radial profiles which approach a parabola at high enough gas superficial velocities.

Degaleesan's CARPT studies had sufficient duration to generate good statistics in all the "cells" for the 3D cell network representing the column. Histograms, *i.e.* probability density functions for various instantaneous velocity components, are presented in Figure 5 for representative compartments (cells) located at various radial positions at axial elevation of 70 cm above the distributor and in the azimuthal plane of $\theta = \pi/2$. Radial and azimuthal velocity components seem normally distributed with the mean of zero, while axial components have a positive or negative mean depending on the radial position. It is noteworthy that the magnitude of the instantaneous velocities can be orders of magnitude higher than the mean. Reynolds stress profiles and kinetic energy due to velocity fluctuations were also computed throughout the column. The nine components of the stress tensor (*i.e.* six since due to symmetry three are the same), averaged over the region of the column with negligible radial and azimuthal mean velocities, indicate that the axial normal stress, τ_{zz} is about two times higher than the radial, τ_{rr}, or azimuthal normal stresses, $\tau_{\theta\theta}$, which are similar in magnitude. All normal stresses are fairly uniformly distributed (except close to the wall) with the axial stress showing a slight peak at mid-radius. The Reynolds shear stress, τ_{rz}, is much lower than the radial or angular normal stresses (typically by a half) and exhibits a peak close to the velocity inversion point, while the shear stresses involving the azimuthal fluctuating velocities τ_{θ}, $\tau_{\theta r}$ and $\tau_{\theta z}$ are negligible and can be taken as zero. Further detailed analysis of the various turbulent parameters and axial liquid velocity profiles as a function of superficial gas velocity and column diameter are discussed elsewhere (Degaleesan, 1997). It should be noted that reasonable confidence can be placed on CARPT results since the comparison of Reynolds shear stress, τ_{rz}, with the results obtained by Menzel *et al.* (1990) using hot film anemometry (HFA) is favorable. Equally favorable is the comparison of other components of the stress tensor close to the wall in bubbly flow at low superficial gas velocity with the measurements of Mudde *et al.* (1992) *via* laser doppler anemometry (LDA). Details of these comparisons are provided by Degaleesan (1997).

The Lagrangian autocorrelation coefficients in radial, azimuthal and axial directions, as well as the cross-correlation coefficients were computed by Degaleesan (1997) from CARPT data. The cross-correlation in the z-θ and r-θ directions are found to be negligible. The components of the eddy diffusivity tensor are evaluated using the equations shown in Table 1. While azimuthal and axial eddy diffusivities reach an asymptotic value after 0.1 to 0.5 s (depending on the radial location), radial eddy diffusivity peaks at 0.05 to 0.2 s. The peak value is 4 to 8 times higher than the asymptotic value. Following Gousbret, Berlemont and Picart (1984) the asymptotic values are used for the azimuthal and axial diffusivities and the peak value for the radial. Thus, for the 14 cm diameter column operated at Ug = 12 cm/s, the eddy diffusivity tensor in the central plane can be represented by:

$$D = \begin{pmatrix} D_{rr} & D_{\theta r} & D_{zr} \\ D_{r\theta} & D_{\theta\theta} & D_{z\theta} \\ D_{rz} & D_{\theta z} & D_{zz} \end{pmatrix} = \begin{pmatrix} 18.1 & 0.0 & 1.20 \\ 0.0 & 54.1 & 0.0 \\ 1.20 & 0.0 & 205 \end{pmatrix} \quad (1)$$

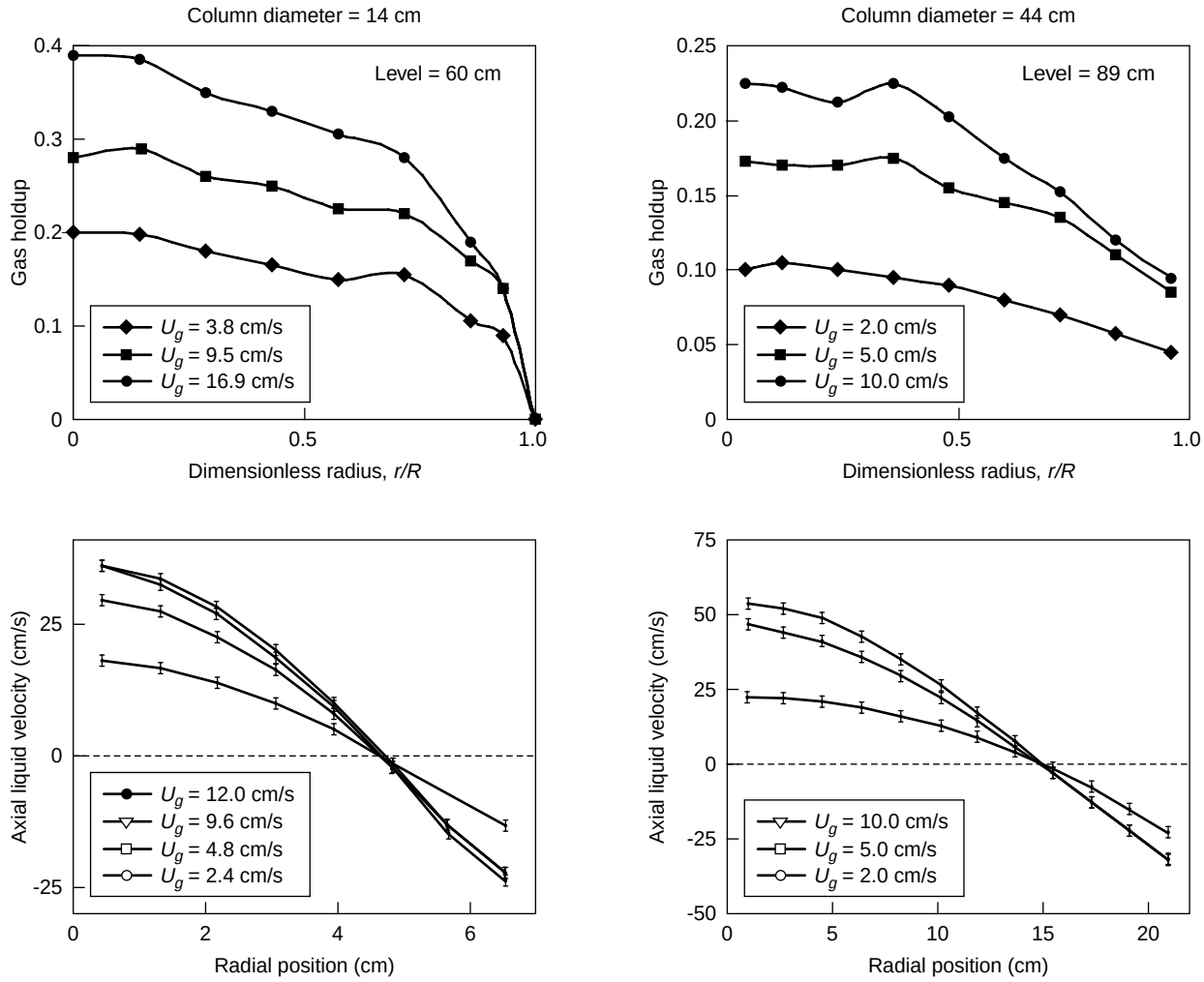

Figure 4

Gas holdup and axial liquid velocity radial profiles as a function of gas superficial velocity.

The components D_{ij} of the diffusivity tensor reported above are in cm^2/s. The behavior of the components along the principal diagonal as a function of radial position and superficial gas velocity is described by Degaleesan (1997). For the purposes of reactor flow pattern modeling it is clearly sufficient to maintain only the principal diagonal components of the eddy diffusivity tensor.

2.1 Utilization of CARPT Data in Prediction of Liquid Mixing and Tracer Responses

We wanted to assess how well can the quantities determined by CARPT-CT be used to describe the liquid flow pattern and mixing in bubble columns. First we wanted to know whether the collected CARPT data can be utilized to predict the liquid flow pattern, such as quantified by an impulse tracer response in a laboratory column characterized by CARPT-CT data. Second, we wanted to know whether these findings can be extrapolated to industrial conditions.

To address the first question, CARPT data was collected in a 8" (0.2 m) diameter column using air-water in churn-turbulent flow at U_g = 10 cm/s. CT scans indicated an axisymmetric holdup distribution which did not change much with height for at least 3/4 length of the column (in the region about one diameter removed from the distributor and from the liquid and free surface). The azimuthally averaged liquid holdup distribution is shown as a function of radius in Figure 6. This holdup distribution drives a large liquid recirculation cell which exhibits the radial profile of the time-averaged liquid velocity shown in Figure 6. The time-averaged radial liquid

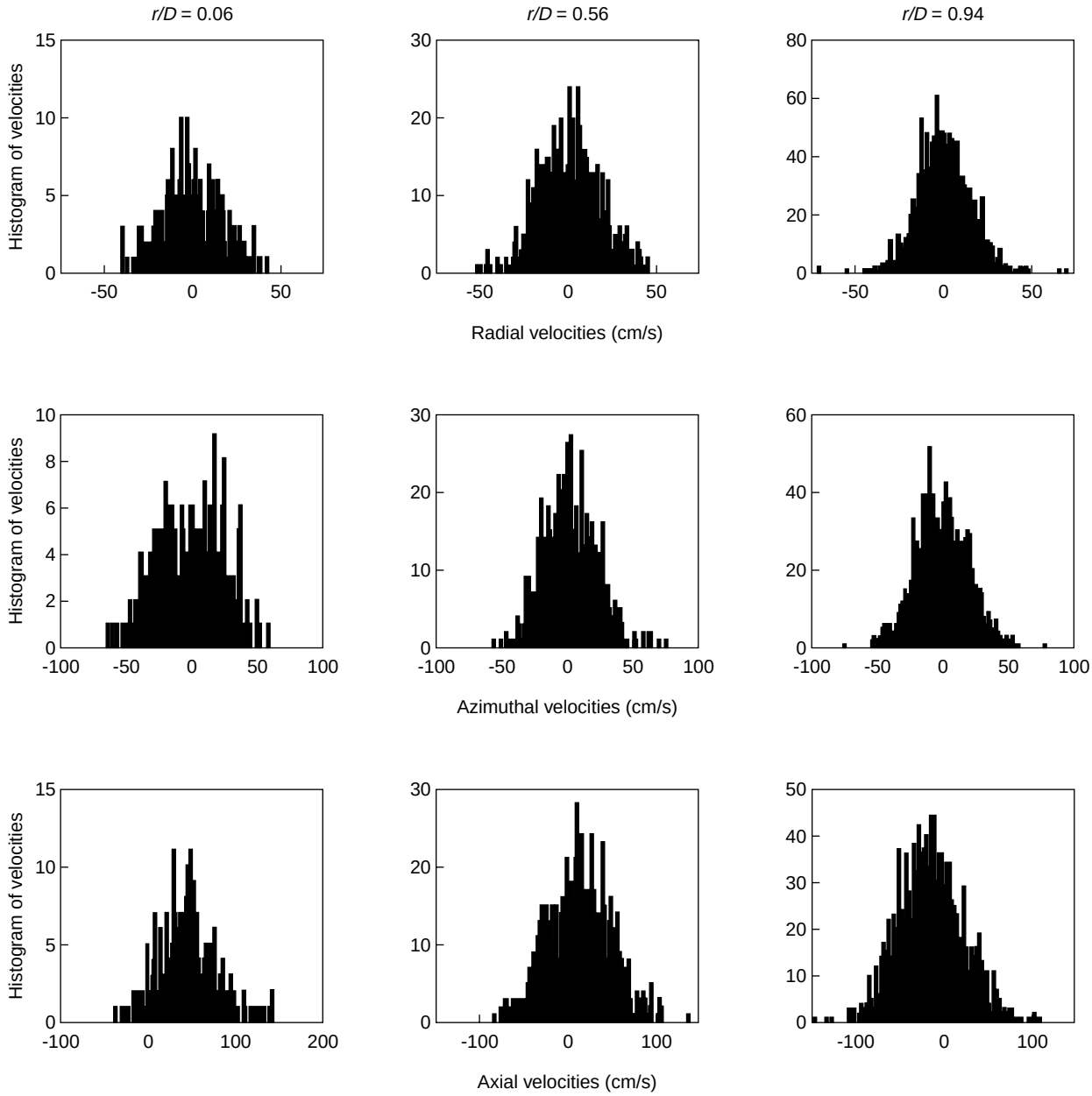

Figure 5

PDF of instantaneous liquid velocities (air-water bubble column: D = 14 cm, U_g = 12 cm/s, z = 70,0 cm).

velocity is essentially zero in this large section of the column where a fully developed axial velocity profile is present. The axial and radial eddy diffusivities, averaged azimuthally and over column height, are shown in Figure 6 also.

Since we have azimuthally averaged the CARPT-CT data we start in our description of the distribution of a nonvolatile liquid nonreactive tracer with the fundamental 2D species conservation equation for the liquid phase. Upon ensemble averaging of this equation we arrive at the convective-diffusion equation (2) shown below:

$$\frac{\partial(\varepsilon_L C)}{\partial t} + \frac{\partial}{\partial z}\,(u_z \varepsilon_L C) = \frac{1}{r}\,\frac{\partial}{\partial r}\left(r\varepsilon_L D_{rr}\frac{\partial C}{\partial r}\right) + \frac{\partial}{\partial z}\left(\varepsilon_L D_{zz}\frac{\partial C}{\partial z}\right) \tag{2}$$

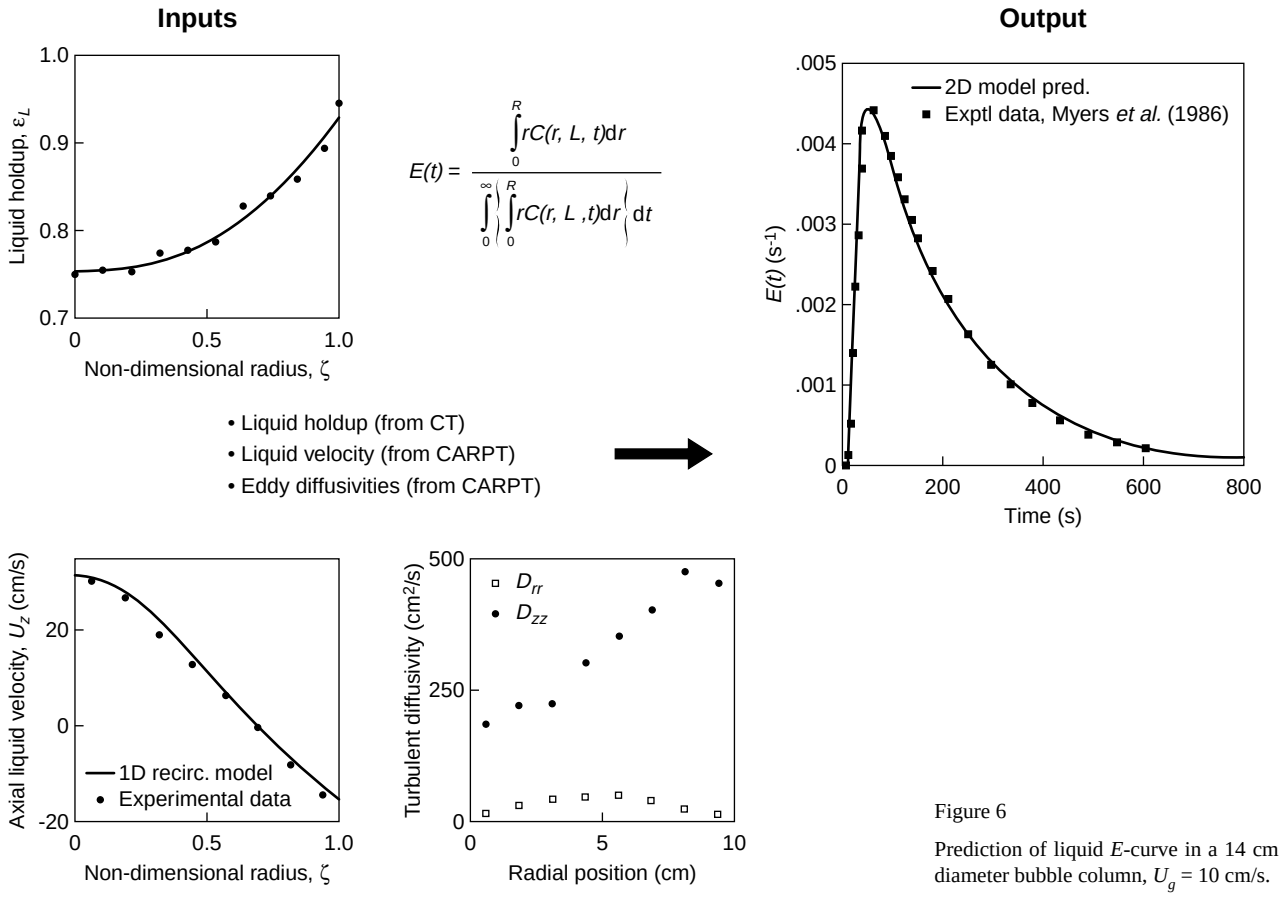

Figure 6

Prediction of liquid *E*-curve in a 14 cm diameter bubble column, U_g = 10 cm/s.

It is noteworthy that the liquid holdup, ε_L, appearing in Equation (2) is precisely the time-averaged liquid holdup determined by CT, while the liquid velocity profile, u_z, is the ensemble average liquid velocity obtained from CARPT. The only assumption involved in arriving at Equation (2) is that the cross-correlation between the fluctuating velocity components and fluctuating tracer concentration can be approximated by Bousinesq approximation with the product of eddy diffusivity and mean velocity gradient. Moreover, we do assume that the eddy diffusivities in the axial and radial directions are those determined by CARPT. At this point, by using in Equation (2) the experimentally determined liquid holdup, $\varepsilon_L(r)$, and liquid velocity profiles, $u_z(r)$, as well as the axial $D_{zz}(r)$, and radial, $D_{rr}(r)$, eddy diffusivity profiles we can solve Equation (2) for the tracer concentration $C(z, r)$ and calculate the mixing cup concentration at the top of the column where liquid outflow is located. Proper normalization of the exit mixing cup concentrations provides the exit age density function for the liquid tracer. Comparison of model-predicted *E*-curve (with no adjustable parameters) with independently determined *E*-curve based on tracer impulse response measurement *(Fig. 6)* indicates excellent agreement (Dudukovic *et al*., 1997).

The success in predicting the *E*-curve (*i.e*. the liquid residence time density) function indicates that our model given by Equation (2) should predict well the behavior of this bubble column for all first-order reactions in the liquid phase. It should also be a pretty good model for mildly nonlinear kinetics. In order to utilize the model at different operating conditions we have developed a scale-up procedure based on the available CARPT-CT data. This procedure allows the estimation of eddy diffusivities and liquid recirculation once the gas holdup profile is known (Degaleesan *et al*., 1997). We have successfully used the model and the procedure for estimation of parameters in describing the tracer data taken in the AFDU at LaPorte. During methanol synthesis a pulse of the liquid radioactive tracer was injected at two various elevations and at two different radial positions and the response was monitored at seven elevations. The ADM cannot distinguish between the two radial injection locations, and while the tracer runs at all elevations can be matched with the ADM, the obtained value of the axial dispersion coefficient varies widely and cannot be predicted. From differential pressure and nuclear densitometry gauge measurements one is able to construct the holdup profile in AFDU at a given operating condition. Using the developed

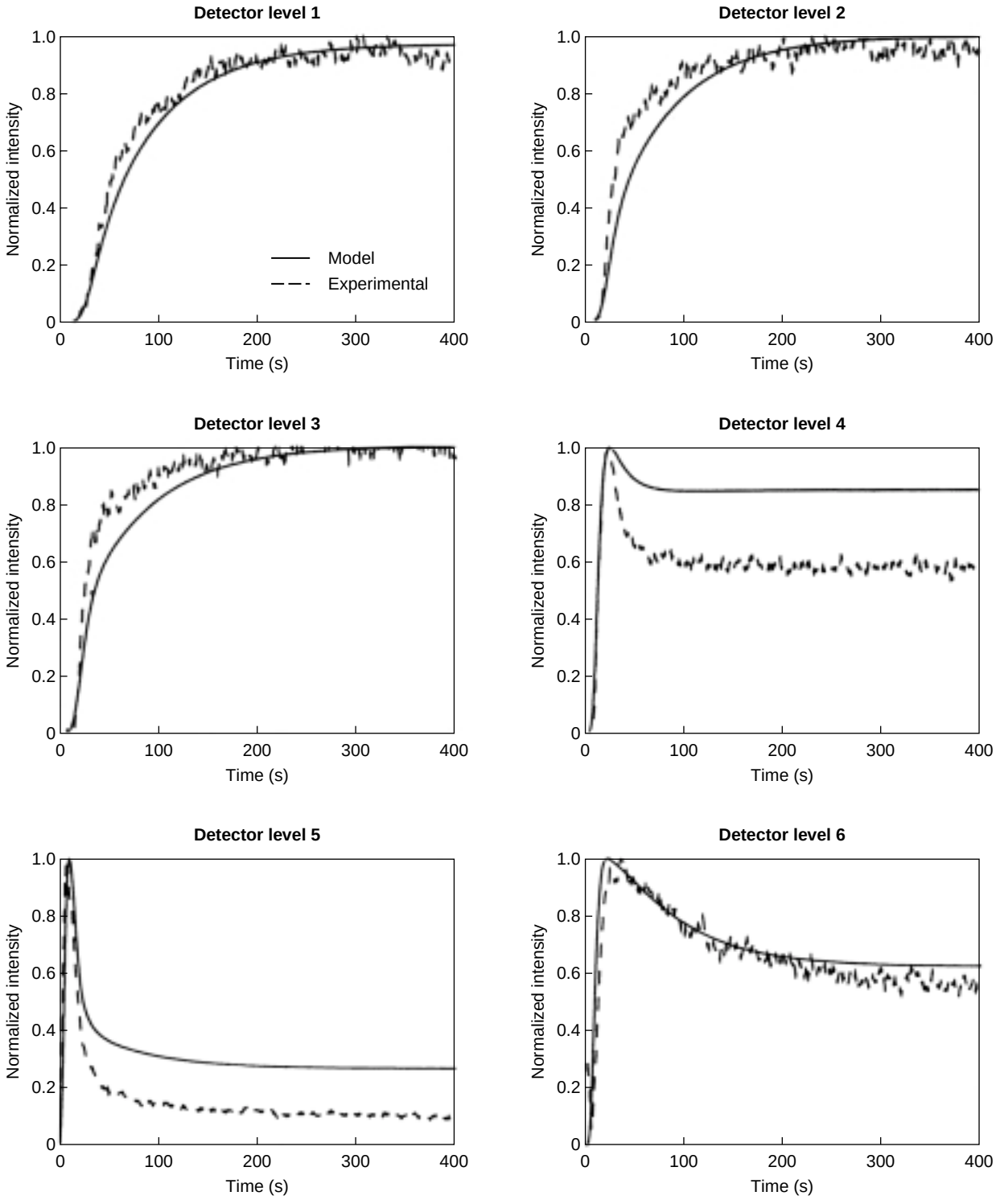

Figure 7

Comparison of experimental (average) tracer responses with 2D model predictions: for wall injection at N1 (run 14.6), U_G = 25 cm/s, T = 250°C, P = 5.2 MPa. (Degaleesan *et al*., 1997.)

procedure liquid recirculation and eddy diffusivities were estimated (Degaleesan *et al.*, 1997). Based on these input parameters tracer responses were predicted at all elevations (with no adjustable parameters) and good agreement with data was obtained *(Fig. 7)*. The remaining discrepancies can be attributed to the imperfections in calibration and execution of the tracer runs. When the ADM is fitted to the tracer responses at various elevations the range of the obtained parameter values is too large to be of help in design. Moreover the tracer responses to injection in the middle of the column and at the wall of the column are distinct and clearly support the liquid recirculation model.

It should be noted that the 2D diffusion-convective model described above can be represented by a simpler two-compartment model for upflow and downflow, with plug flow and axial eddy diffusion in each compartment and cross-flow exchange coefficient (Degaleesan *et al.*, 1996, 1997). This model predicts the *E*-curve almost as well as the results shown here and is easier to use. The design engineer would need to estimate the recirculation rate cross-flow coefficient and eddy diffusivities in each region. Degaleesan and Dudukovic (1998) also show how to relate liquid recirculation and eddy diffusivity to an effective axial dispersion coefficient.

In order to complete a reactor model based on the data base generated by CARPT-CT gas phase flow and mixing models are needed as well as modeling of mass transfer between the gas and the liquid. The framework of our liquid phase mixing model (convection and diffusion) is adopted and augmented by mass transfer and effects of bubble-bubble interactions. In the gas phase model we have developed a procedure to calculate locally the slip velocity and thus construct from the 1D liquid recirculation profile the gas recirculation profile. Following Vermeer and Krishna (1981), Shah *et al.* (1985) and Krishna *et al.* (1999), we assume that in churn-turbulent flow there are large gas bubbles that rise mainly through the middle of the column and small bubbles that rise in the wake of large bubbles but close to the walls are dragged downward by liquid. The large and small bubbles in the central part of the column interact and also exchange soluble components by mass transfer with the liquid that flows upward. The small bubbles can diffuse from the upward to the downward flowing region, and there is mass transfer between small bubbles in the downward flowing region and the liquid in the downflow region. The liquid model was discussed previously. The entry and dis-engagement zones are represented by small stirred tanks. To be consistent with the previously determined liquid flow model the only required input for the gas flow model is the gas holdup profile. All other parameters are calculated either based on theory or from existing correlations in the literature.

At the AFDU in LaPorte gas phase tracer tests were also conducted and gas phase injection was made at the bottom of the column and monitored at several elevations downstream from the point of injection. The ADM again could be fitted to these curves but the axial dispersion coefficient needed to achieve the fits varies widely. The new model predicts the data at various elevations reasonably well, when the bubble-bubble interaction parameter is appropriately chosen. The additional broadening of the experimental curves may be due to problems in interpretation of the measured radioactivity *(Fig. 8)*. The actual tracer concentration curves may be narrower. The investigation of this is in progress. It is of interest to note that if a single size bubble is used instead of large and small bubbles, the model predictions cannot be made to match the data as closely.

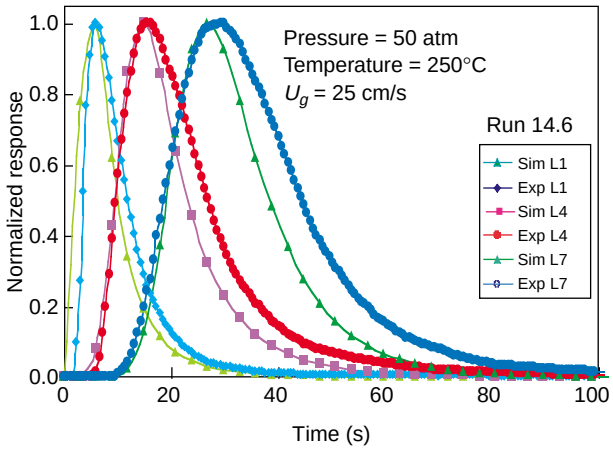

Figure 8

Comparison of simulated and experimental gas phase tracer responses.

The CARPT-CT facility provides us with the opportunity to examine the effect of a number of variables such as presence of internals, solids concentration, pressure and distributor type on holdup and velocity profiles. We have shown that the presence of internals, of the type used at AFDU, does not affect gas holdup profiles significantly in either bubble or churn-turbulent flow (Chen *et al.*, 1998). The liquid velocity profile remains unaffected within the accuracy of the techniques used for its prediction. We have also shown that the behavior of slurries with solids concentrations between 7 to 20% wt is essentially unaffected by the solids concentration as far as slurry recirculation velocity profile and turbulent intensities and stresses are concerned. Research at Sandia National Laboratory confirms that solid particles do not affect much the gas holdup profiles which drive slurry recirculation. Distributor type has no effect on gas holdup profile at U_g = 30 cm/s but does have an effect at U_g = 14 cm/s; however, the industrially important cross and single point distributors still behave the same.

2.2 Comparison of CARPT-CT Data and CFD Predictions

Early on we attempted with our German and Russian colleagues to verify the Eulerian-Lagrangian code in 3D (Devanathan *et al*., 1995) with CARPT data for bubbly flows. Impressive pictures of swirling bubble rich regions were produced that qualitatively looked very much like our visual observations of the column. Moreover, particle trajectories computed by the code looked very much like CARPT trajectories. Even the mean square distance traveled by the particle was comparable between computations and experiments. While time-averaged liquid velocity patterns were comparable, holdup profiles were not. Moreover, the code is not really predictive since it has a tunable parameter in the diffusion type equation for gas holdup.

Recognizing that Lagrangian-Euler approach at present is not sustainable for computation of churn-turbulent flows in large columns, now in CREL we use the CFDLIB codes of Los Alamos, based on the *k*-fluid model, and FLUENT codes based on the two-fluid model and algebraic slip mixture model (ASMM), to compute flow fields in multiphase systems. In the past we have shown qualitative comparisons with 2D experiments using 2D codes (Kumar *et al*., 1994b, 1995b) as well as fully quantitative comparison (Pan, Dudukovic and Chang, 2000). In our computations we utilize the standard formulation for the drag, and base the drag coefficient on the assumed uniform bubble diameter. Classical formulations for the lift and added mass forces are used with standard coefficients. Gas phase turbulence is neglected and liquid phase turbulence is modeled *via* closures of increasing complexity from Prandtl mixing length to *k*-ε models. We had reasonable success in matching quantitatively some 2D data in bubbly flow where liquid turbulence models were found to be unnecessary and drag formulation based on single bubble diameter of 0,5 cm seemed adequate.

Here we compare the axisymmetric 2D CFDLIB code predictions for time-averaged gas holdup and liquid velocities and the data collected in a 3D column operated in the churn-turbulent regime. The experiments were performed by CARPT-CT at CREL in a 3D, 19 cm diameter column with air-water at atmospheric pressure with batch liquid at air superficial velocity of 12 cm/s. A perforated plate distributor with 0.1% total open area, with holes in a square pitch of 1,25 cm and hole diameter of 0,033 cm was used. Static liquid height was 95 cm.

A 2D axisymmetric simulation was performed with the CFDLIB codes. Symmetry at the centerline and free slip at the wall for gas were used as boundary conditions. Atmospheric pressure was specified at the free surface. Free slip for liquid at the distributor was used while inflow gas conditions were prescribed. The following parameters were used for various closure forms: bubble size of 0,5 cm, constant liquid phase mixing length of 1,5 cm, gas-liquid drag coefficient of 0.44, lift coefficient of 0.01, and added mass coefficient of 0.5. The results were significantly sensitive only with respect to bubble size and clearly the selected 0,5 cm represents some hypothetical mean size since most likely the actual bubble size distribution is bimodal.

Figure 9a shows the comparison of predicted and CARPT measured time-averaged liquid velocities at a particular axial location. The agreement is very good, including the prediction of the inversion point for the velocity profile. Figure 9b illustrates the comparison between the predicted gas holdup profile and the one measured by gamma ray tomography. Clearly, the simulation vastly underpredicts the holdup magnitude and distorts (flattens) the holdup profile shape. The simulation also underpredicts the overall holdup (0.12 *versus* measured 0.20). If the flat and low in magnitude gas holdup profiles, predicted by the 2D CFDLIB code, are used with the liquid mixing length of 1,5 cm, which was assumed in the code, in the combined one-dimensional momentum balance for the two phases (Kumar *et al*., 1999), the calculated liquid velocity is much lower than the experimentally observed or 2D model predicted ones. This points to two possible reasons for the discrepancy in measured and predicted holdups. Most likely the interface momentum transfer terms are not modeled correctly and, hence, expressions for drag, lift and added masses need further attention. None of these appear in the 1D model for the combined two phases. The other possibility is that in spite of axial symmetry a 3D flow pattern cannot be adequately captured by a 2D simulation. Evidence for the latter is provided by the recent work of Sokolichin and Eigenberger (1999).

In assessing CFD approaches that seem feasible to use in a large scale bubble column at high volume fraction of the dispersed phase (*i.e.* in churn-turbulent flow) we concluded that only the *k*-fluid Euler-Euler model, or possibly a modified mixture model, have this capability. Since FLUENT provides both codes we used them and in the process verified the computation presented by CFDLIB. In the two-fluid approach, phases are treated as interpenetrating media and the coupling between phases is expressed by a drag which is a function of the local slip velocity. Liquid phase turbulence can be modified *via* the modified *k*-ε model and this is the approach we took when using FLUENT. The mixture model applies the mass and momentum balances to the mixture, assumes local terminal slip between phases and solves for the volume fraction of the dispersed phase while using the *k*-ε model for the mixture. The slip velocity has to be modeled, *i.e.* closure is required. The axial ensemble average liquid velocity profile obtained by CARPT in a 3D column is well predicted by the two-fluid model 2D simulation at low superficial gas velocity (*i.e.* in bubbly flow). In churn-turbulent flow both models overpredict the magnitude of liquid velocity by as much as 30% *(Fig. 10)*. Gas holdup

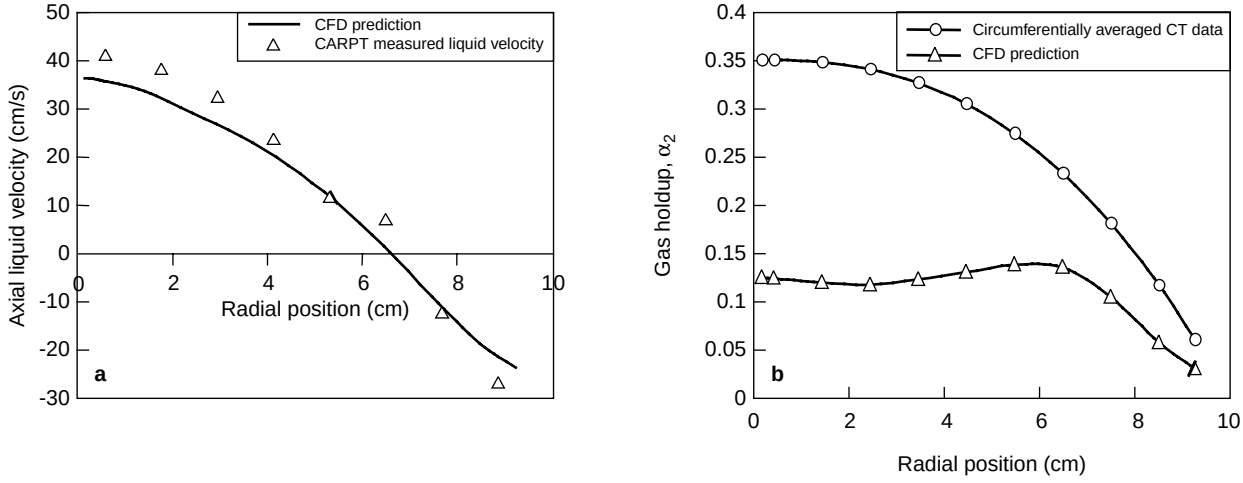

- **3D experimental data from a cylindrical column (19 cm diameter)**
- **2D axisymmetric simulation using CFDLIB**
- **Perforated plate distributor (0.1% open area, 0.33 mm holes)**
- **Superficial gas velocity (12 cm/s)**
- **Mixing length (1.5 cm), bubble diameter (0.5 cm)**
- **Drag coefficient, C_D = 0.44, virtual mass coefficient, C_{VM} = 0.5**

Figure 9

Comparison of CFDLIB two-fluid model 2D simulations for liquid velocity and gas holdup with CARPT-CT data.

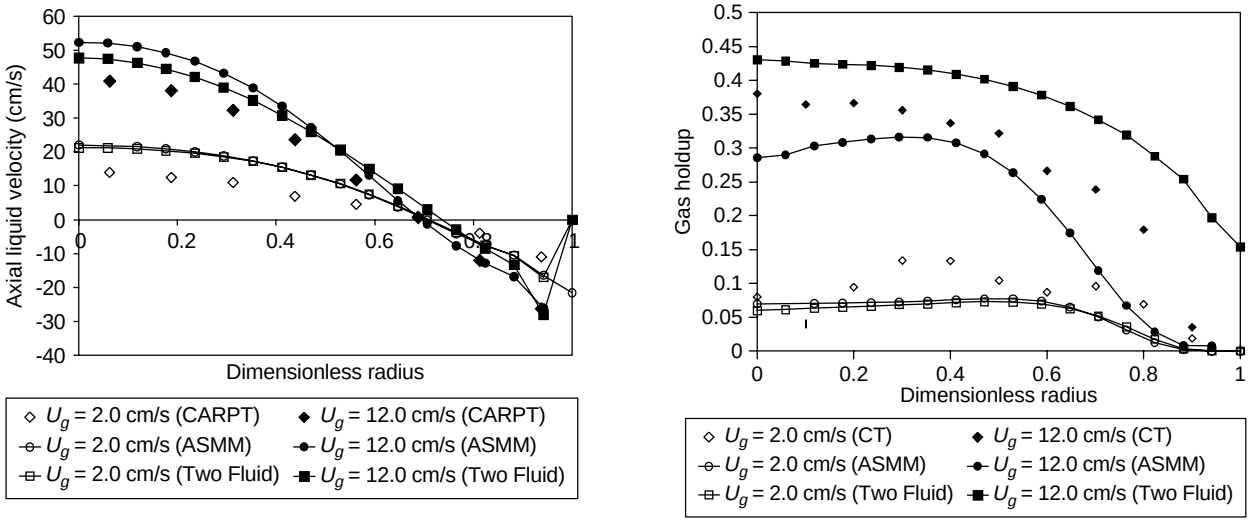

Figure 10

Comparison of FLUENT (two-fluid and ASMM) 2D simulation for liquid velocity and gas holdup with CARPT-CT data.

profile predictions are not very good but the two models bracket the observed holdup profile in churn-turbulent flow (Sanyal *et al*., 1999). The phenomena occurring in the bubble column are clearly three-dimensional as indicated by CARPT and shown by a 3D two-fluid model computation of instantaneous velocity vector and holdup profiles. Instantaneous holdup contours also confirm the presence of transient rapidly changing flow structures and spiral flows, 3D simulation with both the two-fluid model and the mixture model yields good predictions of liquid ensemble average axial velocity profile. The holdup profile is predicted somewhat better with the 3D simulation but is now underpredicted by both models (Sanyal *et al*., 1999). It is noteworthy that a single bubble class was used here for drag representation. The two-class bubble approach will be tried, as it is claimed to yield somewhat better agreement (Krishna *et al*., 1999).

In summary, we have shown here that we are well along our way to meeting the originally set objectives for a better description of the flow pattern in bubble columns:

1 CARPT-CT have proven to be invaluable tools for obtaining velocity, backmixing and holdup information throughout the column;
2 the data base obtained from CARPT-CT has allowed us to establish an improved engineering model for liquid and gas backmixing in bubble columns and to test the CFD codes;
3 we have developed an engineering model firmly based on the observed phenomena for liquid recirculation and gas flow and backmixing. Parameters of this model are tied to first principles as much as possible;
4 2D and 3D CFD computations are starting to yield results which are comparable to experimental observations. A search for reliable models and closures continues.

When we embarked on this endeavor the state of the art of bubble column reactor flow pattern modeling was at level 1, based on assumption of ideal flow patterns with no distinct features of the column behavior. We have elevated the understanding of bubble column hydrodynamics to level 2 at which the key physical features of the buoyancy driven two-phase flows are captured. Now we have to have the opportunity to elevate the state of the art to the predictive level 3.

3 LIQUID-SOLID RISER

Cocurrent upflow of liquid and solids in a dense liquid-solid riser configuration is attracting increased attention for potential solid acid catalyzed alkylations and other applications. Normally this reactor configuration is used when the solid catalyst does deactivate relatively rapidly (*i.e*. on the time scale of the mean residence time in the process) so that continuous solid catalyst regeneration is required. For proper reactor sizing and selection of optimal operating conditions it is necessary to assess and quantify the deviation of the solids phase flow pattern from plug flow and as a function of operating conditions. The process engineer needs to know the extent of solids backflow, if any, and the extent of solids backmixing. We have recently demonstrated (Roy *et al*., 1997, 1999) that CARPT-CT can provide this information. An 8 ft (2.4 m) tall, 6 (0.15 m) in diameter liquid-solid riser was operated in a closed loop with glass beads 2,5 mm in diameter at three solids/liquid loadings and at different liquid superficial velocities. CT scans reveal solids density profiles independent of axial elevation indicating fully developed solids flow *(Fig. 11)*. There is a slight radial solids concentration profile with somewhat increased solids concentration at the wall. However, the radial solids holdup profile is close to linear or parabolic in character and very different from the solids radial concentration profile in gas-solid risers where a lean core and dense solids thin layer at the wall are observed. Typical CARPT results for the ensemble and azimuthally averaged solids velocities at these elevations confirm that the flow is fully developed as the radial profile of the axial solid velocity depends only on liquid superficial velocity and solids loading *(Fig. 11)*. Large scale solids turbulence parameters, such as axial and radial RMS velocities and kinetic energy of turbulence, are also obtained by CARPT as well as solids eddy diffusivities (Roy *et al*., 1999). By monitoring each time of entry of the radioactive tracer particle into the riser and each time of exit from the riser, by two strategically positioned scintillation detectors during the CARPT run, one obtains as a bonus the residence time distribution of the solids on the riser. The mean solids residence times calculated directly from the solids residence time distribution (RTD) and obtained from CT determined solids inventory and CARPT determined velocity profile are in agreement within 10%. This slight deviation is understandable since solids holdup and velocity profiles in the entry and exit zones were not measured.

Experimental evidence gathered by CARPT-CT clearly indicates that in a time average sense there is solids backflow by the wall. There is also solids backmixing by axial diffusion-like mechanism and solids exchange between up and down flowing streams by radial eddy diffusion. These findings are summarized in Table 2. The engineering model that emerges as most appropriate for quantification of these observations is again the upflow-downflow model with axial dispersion and exchange, which is analogous in form to that developed for the bubble column. The experimental results indicate very clearly that solids are not in plug flow, that there is a backflow of solids by the wall and considerable mixing between upward and downward flowing solids.

A mechanistic model attempting to capture the flow pattern in liquid-solid systems (also gas-solid systems) with fidelity should incorporate the following effects:

1 interactions between particles and liquid resulting from the difference between their mean velocity fields, that

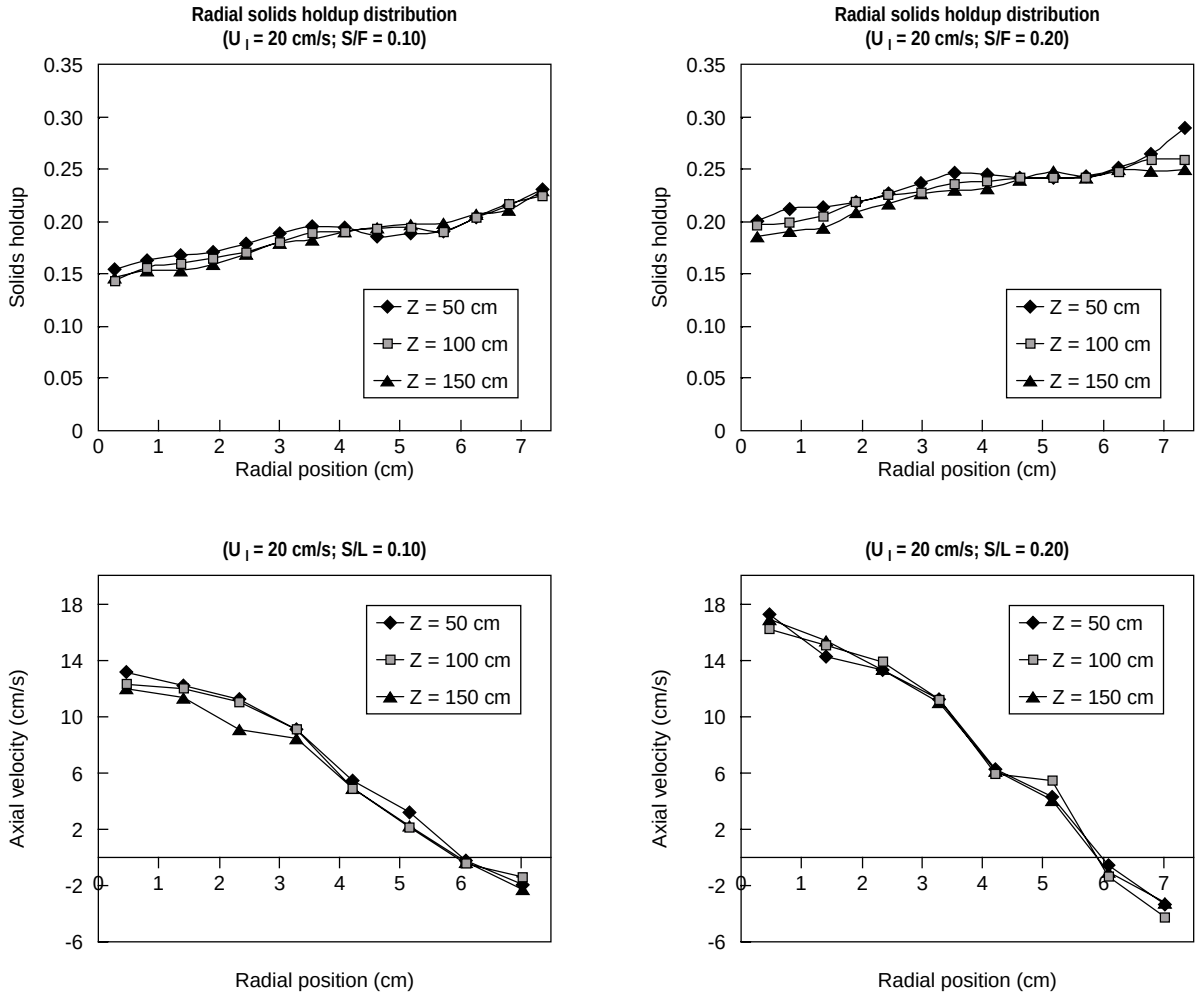

Figure 11

Solids holdup and axial velocity radial profiles obtained by CT-CARPT (S/L is the solids/liquid volume ratio).

TABLE 2

Phenomenological model parameters for liquid-solid riser

Liquid superficial velocity, cm/s	Solids /liquid flow ratio	Net solids flow rate, gpm	Solids upflow rate, gpm	Solids downflow rate, gpm (% of upflow)	Core axial diffusivity, cm^2/s	Annulus axial diffusivity, cm^2/s	Exchange coefficient *(K)*, cm^2/s
15	0.10	3.95	4.36	0.41 (9.4)	105	101	37
	0.15	6.21	6.74	0.53 (7.8)	173	159	45
	0.20	6.67	7.63	0.96 (12.6)	517	498	47
20	0.10	5.18	5.65	0.47 (8.3)	208	193	49
	0.15	7.88	8.81	0.93 (10.6)	397	382	47
	0.20	9.68	10.9	1.22 (11.2)	624	605	56
23	0.10	6.93	7.66	0.73 (9.5)	345	329	54
	0.15	9.21	10.3	1.06 (10.3)	597	581	61
	0.20	10.7	11.9	1.20 (10.1)	889	867	65

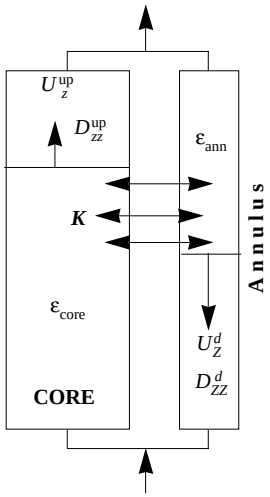

gives rise to the drag force that drives the non-random part of the particle motion;

2 interactions between the particles with the fluctuating components of liquid velocity, which leads to particle diffusion in the liquid field and induces a flux of kinetic energy between the fluctuating velocities of the two phases;

3 interactions within the particle velocity field between the mean and fluctuating components. These generate stresses in the particle assembly and give rise to solids phase pressure and viscosity;

4 interactions between the mean velocity field of the liquid phase and the fluctuating liquid velocity. This gives rise to liquid phase Reynolds stresses which dissipate the turbulent kinetic energy within the liquid phase.

An analysis to decide which of the above effects are important can be based on the work of Bagnold (1954) who formulated a dimensionless group (inertial force/viscous force: so it is like a particle scale Reynolds number in a suspension):

$$\mathrm{Ba} = \lambda^{1/2} \frac{d_p \rho_p}{\mu} \left(\frac{\mathrm{d}U}{\mathrm{d}y} \right) \tag{3a}$$

$$\lambda = \frac{1}{\left(\frac{\alpha_{\max}}{\alpha} \right)^{1/3} - 1} \tag{3b}$$

When Ba < 40 the "macroviscous" regime prevails and the phenomena outlined above as 1, 4 (and 2) are important. When Ba > 450 the " grain-inertia " regime is encountered and phenomena 1, 3 (and 2) are important.

In the riser studied, the mean velocity gradient in the solid phase and the volume fraction α (hence, λ) can be estimated *a priori* from CARPT and CT measurements. The values of Ba thus obtained are of the order of 100. This indicates that of the above cited phenomena 1 to 4 are important.

Thus, a model in FLUENT was formulated accounting for:

- liquid-solid drag (interaction of the mean velocity fields);
- kinetic theory of granular flow for solids phase stresses and pressure. This involves the solution of an equation for pseudo-thermal energy, which along with the terms for solids phase energy transport, also incorporates a term for interaction between the solids phase fluctuations and liquid phase fluctuations;
- a *k*-ε model modified for presence of non-deformable solid particles. This accounts for dissipation of turbulent energy in the liquid phase and also dispersion of particles by the turbulence field;
- a wall boundary condition that accounts for a balance of pseudo-thermal energy of the solids phase: hence, a slip velocity can be calculated locally by solution of an algebraic equation (this is analogous to a wall function formulation in continuum framework of turbulence).

The energy budget and transport in the model may be summarized as:

- energy comes into the system with the liquid;
- drag transfers energy from the mean liquid field to the mean solids field;
- fluctuating solids field extracts energy from the mean solids field (as well as fluctuating liquid field) and eventually dissipates it through collisions between particles, and collisions between particles and wall;
- fluctuating liquid field extracts energy from the mean liquid field and dissipates it eventually. This is modeled by a single length scale (even though in reality it involves a complex cascading phenomenon) with the *k*-ε model;
- the molecular viscosity of liquid also dissipates energy but this effect is much smaller than both turbulence and collisional dissipations;
- eventually both solids and liquid leave the system with some developed mean velocity fields, but the liquid has lost a significant part of its energy in the above dissipation processes.

In the simulations (since the particle size is fixed), the only adjustable parameter is the restitution coefficient (there is no hypersensitivity, as earlier reported by Pita and Sundaresan (1993), and which has been shown to be numerical artifacts). Thus, by varying the restitution coefficient, it is possible to get a good match of the mean solids velocity and volume fraction profiles *(Fig. 12)*. It was found that reasonable downflow velocities could be obtained only by using the appropriate wall boundary condition for predicting the solids slip velocity at the wall. Comparison of the second-order correlations, *i.e.* turbulent kinetic energies, shows order of magnitude agreement when calculated from the model and data. The solids curves predicted by the above simulation are in close agreement with CARPT generated RTDs. This means that to a first-order approximation, the reactor behavior can be modeled based on the above described flow pattern simulation.

4 GAS-SOLID RISER

Gas-solid riser flows are used in catalytic cracking and synthesis of chemicals. The ability of CARPT to provide information on solids velocities was illustrated by Godfrey, Larachi and Chaouki (1999). A more comprehensive study for full quantification of gas-solid riser flows in validation of various proposed CFD codes is in progress at Sandia National Laboratory as part of the Multiphase Fluid Dynamics Research Consortium. We participate in this large team effort by designing CARPT experiments for measurement of solids velocities in the riser.

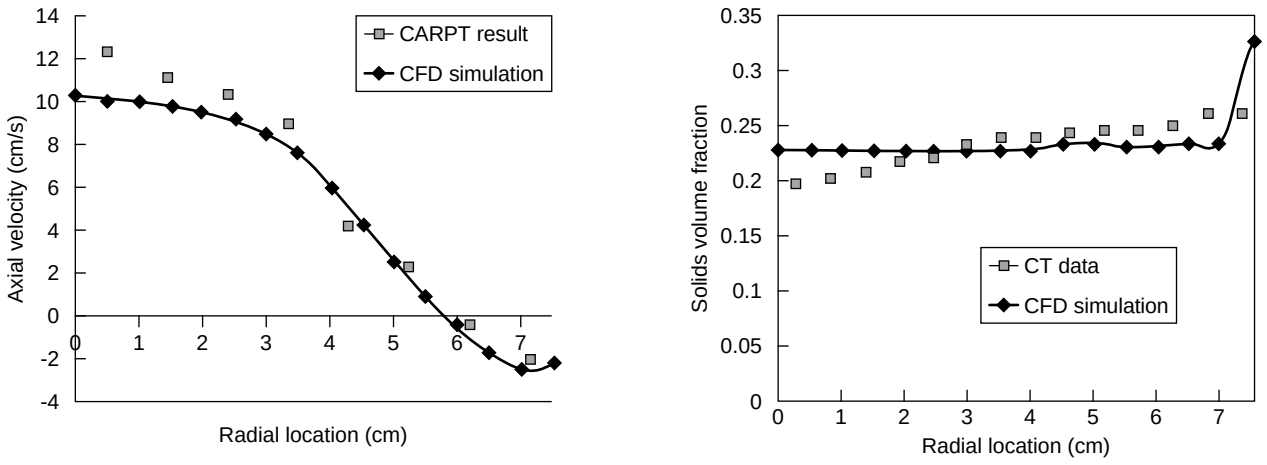

Figure 12

Comparison of FLUENT 2D computations for solids velocity and holdup with data.

5 STIRRED TANK FLOWS

Stirred tank reactors are used in production of polymers, paints, pharmaceuticals, specialty chemicals and other applications. The single-phase flow field in tanks of standard geometry and equipped with standard mixers has been studied extensively. However, multiphase systems which are predominantly encountered in industry have received considerably less attention due to the inability of flow visualization techniques typically employed in single-phase stirred tanks (*e.g.* LDA, PIV, etc.) to obtain reliable results in opaque multiphase flows. CARPT, as already seen, has no such limitations and will be employed for multiphase flows in stirred tanks.

To illustrate the power of CARPT, and also to validate the technique in stirred tank flows, we have performed experiments first in a standard tank with 4 baffles and a 6 blade Rushton turbine impeller at exactly the same conditions at which LDA data were available in water and oil. It should be noted that after a few days needed for calibration of the CARPT detectors all the data was collected in 24 hours while equivalent information takes 6-12 months to obtain by alternative techniques. The insets in Figure 13 illustrate what the CARPT data reveals in complete agreement with previous findings obtained by LDA, PIV and other techniques. Figure 13a shows the CARPT setup for the 8 in (0.2 m) ID tank of height equal to diameter of design that conforms to standard Chapman-Holland type, *i.e.* 4 baffles, 6 blade Rushton turbine with impeller diameter equal to 1/3 of the tank diameter, blade height equal to 1/5 of impeller diameter, and blade width equal to 1/4 of blade diameter. Sixteen detectors were used to monitor the motion of a 2,3 mm neutrally buoyant particle of 80 μCi. Calibration was accomplished by setting the particle at 407 known locations. Figure 13b illustrates the reconstructed particle trajectory during 30 s at 150 rpm. The projection of the particle position on the *r-z* plane is shown. Figure 13c shows the ensemble and azimuthally averaged velocity profile on the *r-z* plane. The tank was divided into 40 cells in the *z* direction, 20 in the *r* direction and 72 in the θ direction, for a total of 57 600 cells with grid size of 5 mm in *r* and *z* directions and 5˚ in the angular direction. Instantaneous velocities are assigned to a cell where the midpoint of two successive particle positions falls. Ensemble averaging and azimuthal averaging yields Figure 13c. Figure 13d displays the projection of the ensemble average velocity vector in the *r-z* plane for the vertical plane that contains the baffles. The strong jet emitted from the impeller and the eye of the loop close to the wall are clearly evident in agreement with the observations reported in the literature (Costes and Couderc, 1988). In Figure 13d the ensemble average velocity vector determined in the impeller midplane and projected on a horizontal plane at that elevation is shown. It is evident that velocity vectors are tangential to the plane of the impeller. A planar jet is the dominant flow feature. In Figure 13e the turbulent kinetic energy is shown in an *r-z* plane containing the baffles. The maximum value of turbulent kinetic energy occurs in the region of the blades and corresponds to about $0.11\,U_{tip}^2$ which is quite comparable to the maximum kinetic energy values reported by LDA measurements which were in the range

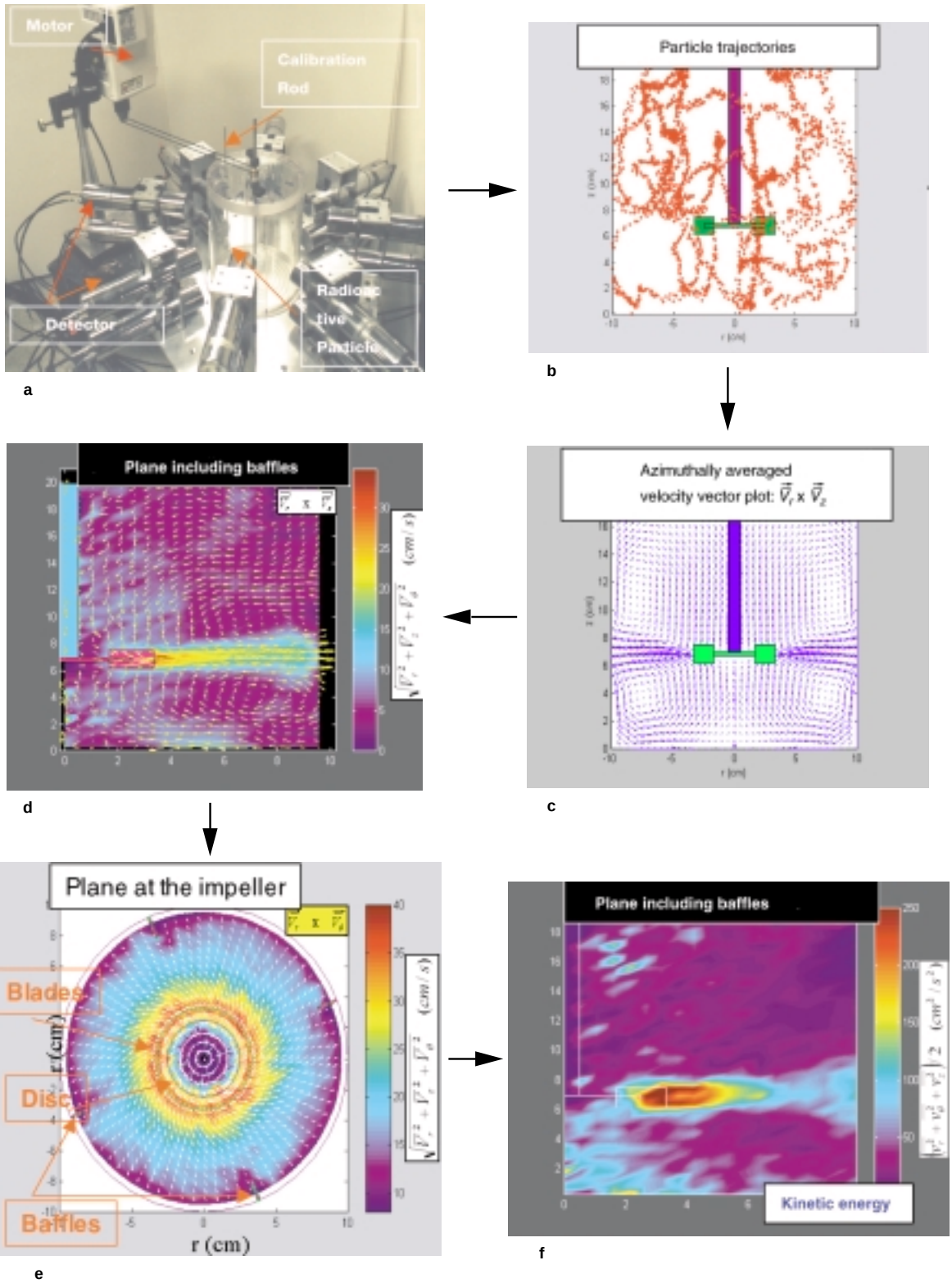

Figure 13
CARPT obtained results in a stirred tank at a glance:
a) Plexiglas stirred tank model and CARPT setup;
b) particle trajectory during 30 s at 150 rpm;
c) averaged velocity field;
d) velocity field and turbulent energy in the vertical plane of the baffles;
e) velocity field and turbulent energy in the horizontal plane of the impeller;
f) kinetic energy in the vertical plane between baffles.

0.12 U_{tip}^2 to 0.14 U_{tip}^2. Figure 14 illustrates that CARPT findings for tangential velocity which are in good agreement with data obtained by other techniques and with CFD simulations (Ranade *et al*., 1999).

This preliminary study (Kemoun *et al*., 1999) of using CARPT in single-phase flows in a stirred tank confirms its ability to provide one with the accurate description of the flow pattern and large scale turbulence caused by energy-containing eddies. As mentioned earlier very fine scale motion is beyond the capability of CARPT to detect.

We plan now mapping of gas-liquid and liquid-solid flows in stirred tanks using CARPT.

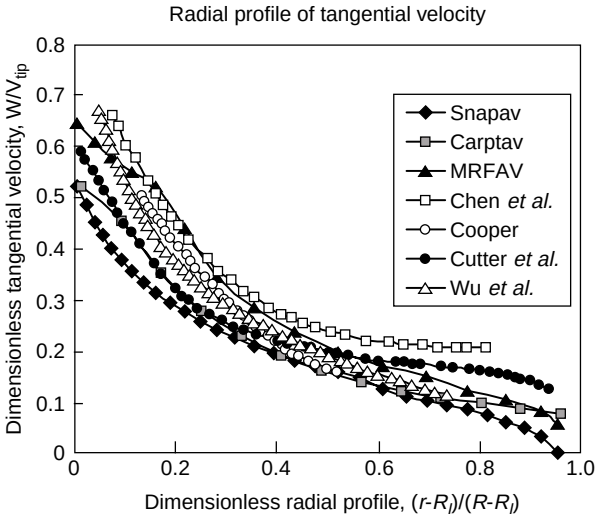

Tangential velocities reported in the literature have maxima varying from 0.6 U_{tip} to 0.8 U_{tip} depending on hub diameter, impeller clearance and angular location. CARPT shows a maximum of 0.60 U_{tip}.

Figure 14

Comparison of experimental and computed radial profiles of tangential velocity.

6 PACKED BEDS WITH TWO-PHASE FLOWS

Packed beds are often the reactor of choice when catalyst activity can be maintained over a long time period (*e.g.* over 6 months) and a flow pattern close to plug flow is desired. Our understanding of trickle-bed reactors has considerably improved during the past decades and this has been summarized in recent reviews (Al-Dahhan *et al*., 1997; Larachi *et al*., 1996). Particle scale incomplete contacting (Al-Dahhan and Dudukovic, 1995, 1996) and its effect on reactor performance for liquid and gas limited reactions has been quantified (Khadilkar *et al*., 1996; Wu *et al*., 1996). The roles of flow direction (*e.g.* upflow *versus* downflow) and use of fines have also been quantified for gas and liquid limited reactions (Wu *et al*., 1996; Khadilkar *et al*., 1996). Recently, one-dimensional reactor scale momentum and species conservation models have been developed coupled with particle scale models that describe transport by Stefan-Maxwell equations. It was shown that such models have the capabilities to describe composition and temperature profiles in the reactor and predict solvent, reactant or product volatilization and reactor dryout (Khadilkar, 1998). Such models are also able to quantify the advantages of reactor operation by cycling the liquid flow rate (Khadilkar, Al-Dahhan and Dudukovic, 1999).

One of the unresolved issues with large scale trickle beds is the accurate prediction of pressure drop, liquid holdup and flow distribution. On one hand neural net based correlations which incorporate fundamentally based mechanistic models are being tried for prediction of global parameters such as pressure drop, holdup, etc. (Iliuta *et al*., 1999). On the other hand it was shown that beds with the same mean voidage but different voidage distributions could cause different liquid and gas flow patterns, some of which lead to flow maldistribution (Jiang *et al*., 1999).

Our effort in this area is focused on obtaining a statistical description of the voidage distribution in the bed packed in a certain manner by a specific packing. Here emission or transmission tomography of accuracy higher than our current setup is needed for experimental validation of the porosity distribution in the packing. Several techniques claim success with imaging of packed and trickle beds (Kantzas, 1994; Reinecke *et al*., 1998; Sederman *et al*., 1998). CFD codes are then used to generate the most likely flow pattern and its possible deviations and this in turn represents the basis for the cell model which can then be used for kinetic-transport calculations and evaluation of reactor performance.

Recently, monoliths have received increased attention for two-phase flow applications. Excellent mass transfer to the walls of the monolith channel can be achieved in the Taylor bubble regime. It is not known, however, to what precision must the distributors be designed to maintain uniformity of behavior in monolith channels, especially for large diameter monoliths. It is also uncertain what happens to the flow due to slight misalignment of monolith channels when monolith blocks are stacked axially and laterally in large vessels. Accurate emission or transmission tomography has the potential to address and answer these questions.

Flow pattern identification in packed beds or monoliths with two-phase flow is difficult as CARPT cannot be used due to potential entrapment of the particle in the bed. NMR can provide the answer only in small diameter vessels. Positron emission tomography and SPEC gamma cameras show promise but have limitations in equipment size that can be viewed. Only radioactive or other tracers, by providing the overall RTD of the phase traced, can address the issues of gross flow maldistribution in packed beds or monoliths.

7 TROUBLESHOOTING *VIA* TRACERS

Often the reactor scale is too large or the process conditions are such that it is not practical to implement the flow visualization techniques discussed earlier. Yet, the information on the overall flow pattern is needed. Sometimes a response to a tracer impulse injection is monitored to confirm or quantify a flow pattern model or CFD calculation, most frequently it is practiced as a troubleshooting tool for identification of possible flow maldistribution, stagnant zones or bypassing. The literature on the use of tracers is broad and rich, with hundreds of papers appearing in just the last few years, and a comprehensive review of this vast field is beyond the scope of this paper. While significant information about the process can be revealed by pseudo-random disturbances of the feed and cross-correlations with appropriately selected output signals, in practice the classical single impulse response technique is most often practiced. Radiotracers are usually employed in industrial practice. The theory of residence time distribution is well developed for single-phase flow systems and its proper extension to multiphase flows has been well described (Nauman, 1981; Aris, 1982; Dudukovic, 1986; Shinnar, 1987). Software packages have been written for interpretation of the impulse response curves (*IAEA*, 1996). Nevertheless, more attention must be paid to the protocol for tracer injection, and especially to the modeling of the tracer response so that one can arrive from the count rate measured by the detectors to the proper description of the mixing cup tracer concentration which is needed for RTD evaluation. An excellent review of the state of the art was recently provided by Blet *et al.* (1999). In addition to the impulse response technique, described in this paper with regard to the bubble column example, encapsulated radioactive sources are used for gamma densitometry. Unfortunately, lack of sufficient demand has so far prevented the development of accurate tomography systems for scanning of industrial reactors. Some advanced research laboratories like *Institut français du pétrole (IFP)* have such units.

It is difficult to give examples of tracer use in industry in troubleshooting applications because such studies are almost invariably proprietary. This makes the tracer studies executed at AFDU in LaPorte under Department of Energy funding so much more valuable. In closing, it should be pointed out that tracers in troubleshooting applications in industry continue to be used in flow measurement, identification of flow pattern and the degree of backmixing, and in estimating the contacting pattern and rate of transport between phases.

SUMMARY AND CONCLUSIONS

Experimental techniques based on radioisotopes provide the information needed for better understanding of phase holdups and flow distribution in multiphase opaque systems. This information is valuable in developing improved, physically based models of the flow pattern and mixing in the reactor. The data obtained by these techniques on holdup and velocity vector profiles is invaluable in validation of multiphase computational fluid dynamic codes.

At present, it is possible to establish improved phenomenological models for bubble columns, risers, stirred tanks and packed beds with two-phase flow, which can describe quantitatively the deviation from usually assumed ideal flow patterns. This can lead to more accurate prediction of reactor performance.

Currently computational fluid dynamic codes cannot predict precisely the observed velocity and phase holdup distributions in multiphase systems but do provide useful insights and semiquantitative guidance. Validation of the codes against data collected by noninvasive means, as described in this paper, contributes to steady improvement in the predictive capabilities of these codes. In packed beds the codes are capable of providing a reasonable assessment of two-phase flow distribution which can be used in reactor performance simulation.

Radioactive tracers and other flow followers remain useful in troubleshooting and assessment of the overall flow pattern.

ACKNOWLEDGMENT

Development of CARPT-CT required a team effort since these are not off-the-shelf techniques. Many individuals contributed extensively to this effort. Among them the following deserve special recognition. Narsi Devanathan established new hardware for CARPT for bubble column studies. Yubo Yang wrote novel software programs for CARPT data acquisition and processing and brought novel interpretation to the data. B.S. Zou and J.M. Mercier performed the work on small diameter slurry bubble columns. Sailesh Kumar developed both hardware and software for the CREL-CT scanner. Sunun Limtrakul studied extensively ebullated beds. Sujatha Degaleesan implemented the wavelet filtering technique and established a comprehensive data base for bubble columns. Bente Sannaes studied slurry bubble columns. Jinwen Chen studied packed beds, bubble columns with internals, while Shantanu Roy studied liquid-solid risers and established Monte-Carlo procedures for evaluation of CARPT resolution and sensitivity. Yubo Yang and Puneet Gupta developed the new Monte-Carlo program for CARPT calibration. Abdenour Kemoun implemented CARPT on high-pressure bubble columns and with Aravind Rammohan performed the CARPT stirred tank studies. Mohan Khadilkar and Yi Jiang improved substantially the trickle bed models. Boon Cheng Ong studied the high-pressure bubble columns. Special thanks are in order to Muthanna Al-Dahhan for organizing many of the above efforts, to Yu Pan and Shantanu Roy for CFD calculations, and especially to

Bernard Toseland of *Air Product*s for providing the focus for bubble column studies.

We also gratefully acknowledge the support of our industrial sponsors: *Air Products & Chemicals, Bayer, Chevron, DuPont, Eastman Chemicals, Elf, Exxon, ICI, IFP, Intevep, Lummus, MEMC, Mitsubishi, Monsanto, Shell, Solutia, Statoil, Union Carbide* and *UOP* and of the Department of Energy *via* grants DE FG 95 22 PC 95212 and contracts DE FC 95 22 PC 95051.

REFERENCES

Al-Dahhan, M.H. and Dudukovic, M.P. (1995) Catalyst Wetting Efficiency in Trickle-Bed Reactors at High Pressure. *Chem. Eng. Sci.*, **50**, 15, 2377-2389.

Al-Dahhan, M.H. and Dudukovic, M.P. (1996) Catalyst Bed Dilution for Improving Catalyst Wetting in Laboratory Trickle-Bed Reactors. *AIChE J*., **42**, 9, 2594-2606.

Al-Dahhan, M.H., Larachi, F., Dudukovic, M.P. and Laurent, A. (1997) High Pressure Trickle-Bed Reactors: A Review. *Ind. Eng. Chem. Res*., **36**, 8 (special issue in honor of Professor Froment), 3292-3314.

Aris, R. (1982) The Scope of RTD Theory and Residence Time Distribution with Many Reactions in Several Environments, in *Residence Time Distribution Theory in Chemical Engineering*, Petho, A., and Noble, R.D. (eds.), Verlag-Chemie.

Bagnold, R.A. (1954) Experiments on a Gravity-Free Dispersion of Large Solid Spheres in a Newtonian Fluid Under Shear. *Proc. Roy. Soc. Lond*., A225, 49.

Blet, V., Berne, V., Berne, Ph., Tola, F., Vitart, X. and Chaussy, C. (1999) Recent Developments in Radioactive Tracer Methodology. *Applied Radiation and Isotopes*, 51, 615-624.

Chaouki, J., Larachi, F. and Dudukovic, M.P. (eds.) (1997a) *Non-Invasive Monitoring of Multiphase Flows*, Elsevier.

Chaouki, J., Larachi, F. and Dudukovic, M.P. (1997b) Non-Invasive Tomographic and Velocimetric Monitoring of Multiphase Flows. *Ind. Eng. Chem. Research*, **36**, 11, 4476-4503.

Chen, J., Gupta, P., Degaleesan, S., Al-Dahhan, M.H., Dudukovic, M.P. and Toseland, B.A. (1998) Gas-Holdup Distributions in Large Diameter Bubble Columns Measured by Computed Tomography. *Flow Meas. Instr.*, 9, 91-101.

Chen, K.Y., Hajduk, J.C. and Johnson, J.W. (1988) Laser-Doppler Anemometry in a Baffled Mixing Tank. *Chem. Eng. Commn.*, 72, 141-157.

Costes, J. and Couderc, J.P. (1988) Study by LDA of the Turbulent Flow Induced by a Rushton Turbine Flow Induced by a Rushton Turbine in a Stirred Tank: Influence of the Size of the Units-1. Mean Flow and Turbulence. *Chem. Eng. Sci.*, **43**, 10, 2751-2764.

Cooper, R.G. and Wolf (1967), Pumping Capacities in Stirred Tanks—Theory and Application. *Can J. Chem. Eng.*, **45**, 4, 197-203.

Degaleesan, S., Roy, S., Kumar, S.B. and Dudukovic, M.P. (1996) Liquid Mixing Based on Convection and Turbulent Dispersion in Bubble Columns. *Chem. Eng. Sci.*, **51**, 10, 1967-1976.

Degaleesan, S. (1997) Fluid Dynamic Measurements and Modeling of Liquid Mixing in Bubble Columns. *Thesis*, Washington University, St. Louis.

Degaleesan, S. and Dudukovic, M.P. (1998) Liquid Backmixing in Bubble Columns and the Axial Dispersion Coefficient. *AIChE J*., **44**, 11, 2369-2378.

Degaleesan, S., Dudukovic, M.P., Toseland, B.A. and Bhatt, B.L. (1997) A Two Compartment Convective Diffusion Model for Slurry Bubble Column Reactors. *Ind. Eng. Chem. Research*, **36**, 11, 4670-4680.

Devanathan, N., Dudukovic, M.P., Lapin, A. and Lubbert, A. (1995) Chaotic Flow in Bubble Column Reactors. *Chem. Eng. Sci*., **50**, 16, 2661-2667.

Devanathan, N., Moslemian, D. and Dudukovic, M.P. (1990) Flow Mapping in Bubble Columns Using CARPT. *Chem. Eng. Sci*., **45**, 8, 2285-2291.

Dudukovic, M.P. (1986) Tracer Methods in Chemical Reactors. Techniques and Applications, in Chemical Reactor Design and Technology. *NATO Series E: Applied Sciences*, DeLasa, H.I. (ed.) 110, 107-189, Martinus Nkjhoff Publishers.

Dudukovic, M.P., Degaleesan, S., Gupta, P. and Kumar, S.B. (1997) Fluid Dynamics in Churn-Turbulent Bubble Columns: Measurement and Modeling. *ASME FEDSM*, 3517, 1-15, June 22-26.

Godfrey, L., Larachi, F. and Chaouki, J. (1999) Position and Velocity of a Large Particle in a Gas/Solid Riser Using the Radioactive Particle Tracking Technique. *Can. J. Chem. Eng*., 77, 253-261.

Gousbret, G., Berlemont, A. and Picart, A. (1984) Dispersion of Discrete Particles by Continuous Turbulent Motions. *Phys. Fluids*, 27, 827-837.

Grevskott, S., Sannaes, B.H., Dudukovic, M.P., Hgarbo, K.W. and Svendsen, H.F. (1996) Liquid Circulation, Bubble Size Distribution and Solids Movement in Two and Three Phase Bubble Columns. *Chem. Eng. Sci*., **51**, 10, 1703-1713.

Gupta, P. (1998) Monte Carlo Simulations of NaI (T l) Detector Efficiencies for Radioactive Particle Tracking in Multiphase Flows. *Chemical Reaction Engineering Laboratory (CREL) Annual Report*, June 1, 1997-May 31, 1998, 117-122.

IAEA (International Atomic Energy Agency) (1996) Residence Time Distribution Software Analysis. *Computer Manual Series*, **11**.

Iliuta, I., Ortiz, A., Larachi, F., Grandjean, B.P.A. and Wild, G. (1999) Hydrodynamics and Mass Transfer in Trickle-Bed Reactors: An Overview. *Chem. Eng. Sci*., **54**, 21, 5329-5337.

Jiang, Y., Khadilkar, M.R., Al-Dahhan, M.H. and Dudukovic, M.P. (1999) Two-Phase Flow Distribution in 2D Trickle-Bed Reactors. *Chem. Eng. Sci*., **54**, 14, 2409-2419.

Kantzas, A. (1994) Computation of Holdups in Fluidized and Trickle Beds by Computer-Assisted Tomography. *AIChE J*., **40**, 7, 1254-1261.

Kemoun, A., Rammohan, A., Al-Dahhan, M.H. and Dudukovic, M.P. (1999) Characterization of a Single Phase Flow in a Stirred Tank Using Computer Automated Radioactive Particle Tracking. *Mixing XVII, 17th Biennial North American Mixing Conference*, Banff, Canada, August 15-20.

Khadilkar, M.R. (1998) Performance Studies of Trickle Bed Reactors. *Thesis*, Washington University, St. Louis.

Khadilkar, M.R., Al-Dahhan, M.H. and Dudukovic, M.P. (1999) Parametric Study of Unsteady State Flow Modulation in Trickle Bed Reactors. *Chem. Eng. Sci*., **54**, 14, 2585-2595.

Khadilkar, M.R., Wu, Y.X., Al-Dahhan, M.H., Dudukovic, M.P. and Colakyan, M. (1996) Comparison of Trickle-Bed and Upflow Reactor Performance at High Pressure: Model Predictions and Experimental Observations. *Chem. Eng. Sci.*, **51**, 10, 2139-2148.

Krishna, R., Urseanu, M.I., van Baten, J.M. and Ellenberger, J. (1999) Influence of Scales on the Hydrodynamics of Bubble

Columns Operating in the Churn-Turbulent Regime: Experiments vs. Eulerian Simulations. *Chem. Eng. Sci*., **55**, 21, 4903-4911.

Kumar, S.B., Devanathan, N., Moslemian, D. and Dudukovic, M.P. (1994a) Effect of Scale on Liquid Recirculation in Bubble Columns. *Chem. Eng. Sci*., **49**, 24B, 5637-5652.

Kumar, B.S., Moslemian, D. and Dudukovic, M.P. (1995a) A Gamma Ray Tomographic Scanner for Imaging Void Fraction Distribution in Bubble Columns. *Flow. Meas. Instr*., **6**, 1, 61-73.

Kumar, S.B., Moslemian, D. and Dudukovic, M.P. (1997) Gas-Holdup Measurements in Bubble Columns Using Computed Tomography. *AIChE J*., **43**, 6, 1414-1425.

Kumar, S.B. and Dudukovic, M.P. (1997) Computer Assisted Gamma and X-ray Tomography: Applications to Multiphase Flow Systems, Ch. 2, pp 47-103, in Chaouki, J., Larachi, F. and Dudukovic, M.P. (eds.) (1997a).

Kumar, S., Vanderheyden, W.B., Devanathan, N., Dudukovic, M.P. and Kashiwa, B.A. (1994b) Numerical Simulation and Experimental Verification of the Gas-Liquid Flow in Bubble Columns. *AIChE Annual Meeting*, San Francisco, Nov. 14-18.

Kumar, S., Vanderheyden, W.B., Devanathan, N., Dudukovic, M.P. and Kashiwa, B.A. (1995b) Computation of Flow Fields in Multiphase Systems. *Mixing XV, NAMF Conference*, Banff, Canada, June 18-23.

Larachi, F., Al-Dahhan, M.H., Dudukovic, M.P. and Laurent, A. (1996) High Pressure Trickle-Bed Reactors: A State-of-the-Art Review. *Proceedings of the 12th International Congress of Chemical and Process Engineering*, CHISAi12, Prague, Czech Rep., August 25-30.

Larachi, F., Chaouki, J., Kennedy, G. and Dudukovic, M.P. (1997) Radioactive Particle Tracking in Multiphase Reactors: Principles and Applications. Ch. 11, pp. 335-406, in Chaouki, J., Larachi, F. and Dudukovic, M.P. (eds.) (1997a).

Larachi, F., Kennedy, G. and Chaouki, J. (1995) 3-D Mapping of Solids Flow Fields in Multiphase Reactors with RPT. *AIChE J*., **41**, 2, 439-443.

Limtrakul, S. (1996) Hydrodynamics of Liquid Fluidized Beds and Gas-Liquid Fluidized Beds. *Thesis*, Washington University, St. Louis.

Lin, J.S., Chen, M.M. and Chao, B.T. (1985) A Novel Radioactive Particle Tracking Facility for Measurement of Solids Motion in Gas Fluidized Beds. *AIChE J*., **31**, 3, 465-473.

Meek, C.C. (1972) Statistical Characterization of Dilute Particulate Suspensions in Turbulent Fluid Fields. *Ph.D. Thesis*, University of Illinois, Urbana.

Menzel, T., Inderweide, T., Standacher, O., Wein, O. and Onken, U. (1990) Reynolds Shear Stress for Modeling of Bubble Column Reactors. *Ind. Eng. Chem. Research*, **29**, 6, 988-994.

Moslemian, D., Chen, M.M. and Chao, B.T. (1989) Experimental and Numerical Investigations of Solids Mixing in a Gas-Solid Fluidized Bed. *Particulate Sci.: Techn*., **7**, 4, 335-355.

Mudde, R.F., Groen, J.S. and van den Akker, H.E.A. (1997) Liquid Velocity Field in Bubble Columns: LDA Experiments. *Chem. Eng. Sci*., **52**, 21/22, 4217-4224.

Nauman, B.E. (1981) Residence Time Distributions and Micromixing. *Chem. Eng. Communications*, 8, 53-131.

Pan, Y., Dudukovic, M.P. and Chang, M. (1999) Dynamic Simulation of Bubbly Flow in Bubble Columns. *Chem. Eng. Sci*., **54**, 13, 2481-2489.

Pan, Y., Dudukovic, M.P. and Chang, M. (2000) Numerical Investigation of Gas-Driven Flow in Two-Dimensional Bubble Columns. *AIChE J*., **46**, 3, 434-449.

Pita, J.A. and Sundaresan, S. (1993) Developing Flow of a Gas-Particle Mixture in a Vertical Riser. *AIChE J*., **39**, 4, 541-552.

Ranade, V.V., Rammohan, A., Kemoun, A., Al-Dahhan, M.H. and Dudukovic, M.P. (1999) Motion of Neutrally Buoyant Particles in Stirred Vessels: CARPT Experiments and CFD Simulations. *Mixing XVII, 17th Biennial North American Mixing Conference*, Banff, Canada, August 15-20.

Reinecke, N., Petritsch, G., Schmitz, D. and Mewes, D. (1998) Tomographic Measurement Techniques—Visualization of Multiphase Flows. *Chem. Eng. Technol*., **21**, 1, 217-218.

Roy, S., Chen, J., Kumar, S.B., Al-Dahhan, M.H. and Dudukovic, M.P. (1997) Tomographic and Particle Tracking Studies in a Liquid-Solid Riser. *Ind. Eng. Chem. Research*, **36**, 11, 4666-4669.

Roy, S., Kemoun, A., Al-Dahhan, M.H. and Dudukovic, M.P. (1999) Dense Vertical Liquid-Solid Flow in a Riser: Experimental Analysis. *NHTC 99: The 33rd National Heat Transfer Conference*, Albuquerque, NM, August 15-17.

Roy, D., Larachi, F., Lagros, R. and Chaouki, J. (1994) A Study of Solid Behavior in Spouted Beds Using 3-D Particle Tracking. *Can J. Chem. Eng*., **72**, 6, 945-952.

Sanyal, J., Vasquez, S., Roy, S. and Dudukovic, M.P. (1999) Numerical Simulation of Gas-Liquid Dynamics in Cylindrical Bubble Column Reactors. *Chem. Eng. Sci*., **55**, 21, 5071-5083.

Sederman, A.J., Johns, M.L., Alexander, P. and Gladden, L.F. (1998) Structure-Flow Correlations in Packed Beds. *Chem. Eng. Sci*., **53**, 12, 2117-2128.

Shah, Y.T., Joseph, S., Smith, D.N. and Reuther, J.A. (1985) Two-Bubble Class Model for Churn-Turbulent Bubble Column Reactor. *Ind. Eng. Chem. Process Des. Dev*., **24**, 4, 1096-1104.

Shinnar, R (1987) Use of Residence and Contact Time Distributions in Reactor Design, *in Chemical Reaction and Chemical Reactor Engineering*, Carberry, J.J. and Varma, A., (eds.), Marcel Dekker.

Sokolichin, A. and Eigenberger, G. (1999) Applicability of the Standard k-ε Turbulence Model to the Dynamic Simulation of Bubble Columns: Part I. Detailed Numerical Simulations. *Chem. Eng. Sci*., **54**, 13-14, 2273-2284.

Vermeer, D.J. and Krishna, R. (1981) Hydrodynamics and Mass Transfer in Bubble Columns Operating in the Churn-Turbulent Regime. *Ind. Eng. Chem. Process Des. Dev*., **20**, 3, 475-482.

Wu, Y.X., Al-Dahhan, M.H., Khadilkar, M.R. and Dudukovic, M.P. (1996) Evaluation of Trickle-Bed Reactor Models for a Liquid Limited Reaction. *Chem. Eng. Sci*., **51**, 11, 2721-2725.

Yang, Y.B., Devanathan, N. and Dudukovic, M.P. (1993) Liquid Backmixing in Bubble Columns via Computed-Automated Radioactive Particle Tracking (CARPT). *Experiments in Fluids*, **16**, 1, 1-9.

Final manuscript received in December 1999